UNIVERSIDADE FEDERAL DO PARANÁ

HUDSON FRANKLIN PESSOA VERAS

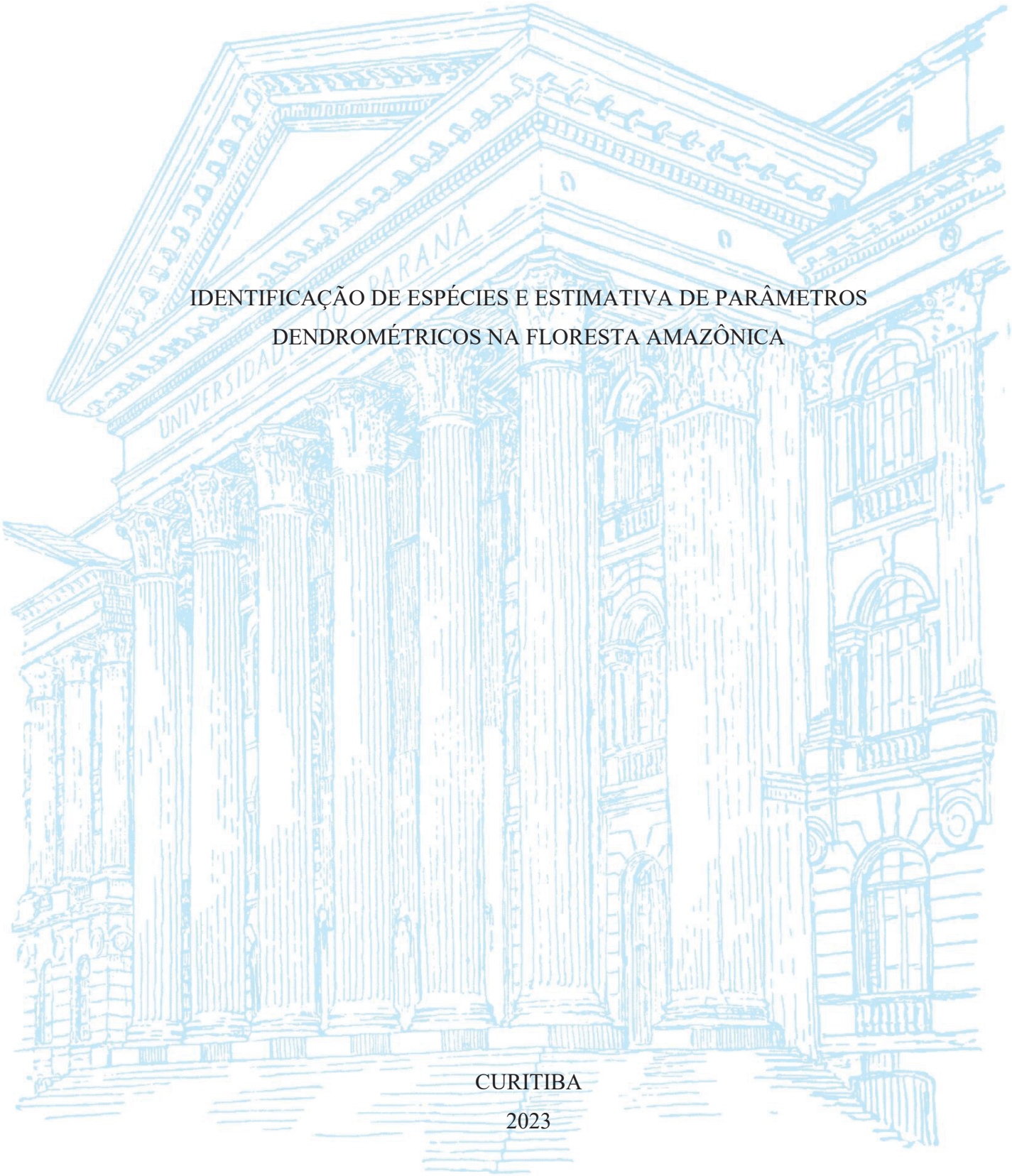

IDENTIFICAÇÃO DE ESPÉCIES E ESTIMATIVA DE PARÂMETROS DENDROMÉTRICOS NA FLORESTA AMAZÔNICA

CURITIBA

2023

HUDSON FRANKLIN PESSOA VERAS

IDENTIFICAÇÃO DE ESPÉCIES E ESTIMATIVA DE PARÂMETROS DENDROMÉTRICOS NA FLORESTA AMAZÔNICA

Tese apresentada ao curso de Pós-Graduação em Engenharia Florestal, Setor de Ciência Agrária, Universidade Federal do Paraná, como requisito parcial à obtenção do título de Doutor em Engenharia Florestal.

Orientador: Prof. Dr. Carlos Alberto Sanquetta

Coorientadores: Prof(a). Dr(a). Ana Paula Dalla Corte, Prof Dr. Evandro Figueiredo Orfanó, Prof. Dr. Matheus Pinheiro Ferreira

CURITIBA

2023

Ficha catalográfica elaborada pela
Biblioteca de Ciências Florestais e da Madeira - UFPR

Veras, Hudson Franklin Pessoa
Identificação de espécies nativas na Amazônia e estimativa de parâmetros / Hudson Franklin Pessoa Veras . - Curitiba, 2023.
1 recurso on-line : PDF.

Orientador: Prof. Dr. Carlos Alberto Sanquetta
Coorientadores: Profª. Drª. Ana Paula Dalla Corte
Prof. Dr. Evandro Figueiredo Orfanó
Prof. Dr. Matheus Pinheiro Ferreira

Tese (Doutorado) - Universidade Federal do Paraná, Setor de Ciências Agrárias. Programa de Pós-Graduação em Engenharia Florestal. Defesa: Curitiba, 20/03/2023.

1. Árvores - Amazônia. 2. Árvores - Identificação. 3. Árvores - Medição. 4. Levantamentos florestais. 5. Florestas - Sensoriamento remoto. 6. Fotografia aérea em florestas. 7. Processamento de imagens. 8. Redes neurais (Computação). .I. Sanquettta, Carlos Alberto. II. Dalla Corte, Ana Paula. III. Orfanó, Evandro Figueiredo. IV. Ferreira, Matheus Pinheiro. V. Universidade Federal do Paraná, Setor de Ciências Agrárias. VI. Título.

CDD - 634.909811
CDU - 634.0.58(811)
528

Bibliotecária: Marilene do Rocio Veiga - CRB 9/424

MINISTÉRIO DA EDUCAÇÃO
SETOR DE CIÊNCIAS AGRÁRIAS
UNIVERSIDADE FEDERAL DO PARANÁ
PRÓ-REITORIA DE PESQUISA E PÓS-GRADUAÇÃO
PROGRAMA DE PÓS-GRADUAÇÃO ENGENHARIA FLORESTAL - 40001016015P0

TERMO DE APROVAÇÃO

Os membros da Banca Examinadora designada pelo Colegiado do Programa de Pós-Graduação ENGENHARIA FLORESTAL da Universidade Federal do Paraná foram convocados para realizar a arguição da tese de Doutorado de **HUDSON FRANKLIN PESSOA VERAS** intitulada: **IDENTIFICAÇÃO DE ESPÉCIES E ESTIMATIVA DE PARÂMETROS DENDROMÉTRICOS NA FLORESTA AMAZÔNICA**, sob orientação do Prof. Dr. CARLOS ROBERTO SANQUETTA, que após terem inquirido o aluno e realizada a avaliação do trabalho, são de parecer pela sua APROVAÇÃO no rito de defesa.

A outorga do título de doutor está sujeita à homologação pelo colegiado, ao atendimento de todas as indicações e correções solicitadas pela banca e ao pleno atendimento das demandas regimentais do Programa de Pós-Graduação.

CURITIBA, 20 de Março de 2023.

Assinatura Eletrônica
22/03/2023 10:10:35.0
CARLOS ROBERTO SANQUETTA
Presidente da Banca Examinadora

Assinatura Eletrônica
22/03/2023 15:57:18.0
VAGNER ALEX PESCK
Avaliador Externo (UNIVERSIDADE ESTADUAL DO CENTRO-OESTE)

Assinatura Eletrônica
23/03/2023 09:51:39.0
SAMUEL DE PÁDUA CHAVES E CARVALHO
Avaliador Externo (UNIVERSIDADE FEDERAL DE MATO GROSSO)

Assinatura Eletrônica
22/03/2023 10:52:37.0
VERALDO LIESENBERG
Avaliador Externo (UNIVERSIDADE DO ESTADO DE SANTA CATARINA)

Assinatura Eletrônica
21/03/2023 18:31:09.0
EVANDRO FERREIRA DA SILVA
Avaliador Externo (UNIVERSIDADE FEDERAL DO PARÁ)

AGRADECIMENTOS

Agradeço à Deus pela vida.

A minha esposa, em especial, Rejane Veras e ao nosso filho (Daniel) que está chegando, por todo amor e apoio incondicional as minhas decisões e barreiras enfrentadas durante toda vida profissional, essencial para alcançar as conquistas e sucesso.

Aos meus familiares, Sr. Joaquim Veras, Srª Maria Pessoa, Kássia Janara, João Paulo e Heloísa Veras, por todo apoio e contribuição constante.

Aos meus orientadores Dr. Carlos Alberto Sanqueta e Drª Ana Paula Dalla Corte por terem me recebidos no Laboratório Biofix e proporcionado uma das melhores experiências acadêmicas já vividas, sentimento de conviver entre amigos e com harmonia, cruciais para formação acadêmica do discente, além dos apontamos cirúrgicos para realização da tese, verdadeiras referencias.

Aos meus coorientadores Dr. Evandro Figueiredo Orfano por ter permitido trabalhar com a base de dados do projeto Geoflora da Embrapa Acre, além das ótimas conversas e trocas de experiências para construção da tese e ao Dr. Matheus Pinheiro Ferreira, em especial, por ter me acolhido e orientado na elaboração da Tese, muito paciente e prestativo, apoio fundamental para realização desse trabalho.

Ao Instituto Federal do Acre, onde sou docente, por permitir a liberação para estudo integral durante o período de estudos da tese, fundamental e essencial.

A Universidade Federal do Paraná por conceder a oportunidade ao acesso gratuito ao ensino de altíssima qualidade.

Ao Programa de Pós-Graduação em Engenharia Florestal (PPGEF) – UFPR pela oportunidade em ingressar e cursar disciplinas internas de excelências com professores únicos essenciais para o desenvolvimento desta pesquisa.

Aos meus amigos e colegas de laboratório do Biofix pela companhia e papos descontraídos, com muita troca de conhecimentos em especial ao irmão Neto Macedo, Manu Guaraná, Iací, Luani, Thiago, Gabriel, Iasmin, Aline, Amanda, Verônica, Augusto, Franciel e Deivison.

Aos amigos do Laboratório do Manejo Florestal pelas ótimas conversas durante o horário do café, uma verdadeira terapia, em especial Jorge, Antônio, Maurício, Clebson, Samuel, Maicon, Brown, Kauê, Diego, Cícero e Lukita.

Ao meu amigo Vinícius, um acreano morando em Curitiba, parceiro de treinos de jiu-jitsu, trilhas e cerveja.

E por fim, à todas as pessoas que contribuíram de alguma forma para finalização do doutorado.

Muitíssimo obrigado!!!

“Acreditar e perseverar, o sucesso virá”

Hudson Veras

RESUMO

O Inventário florestal é um método de levantamento de campo indispensável para conhecer as características quantitativas e qualitativas de uma floresta. Esta atividade em florestas nativas é demorada, onerosa, risco a saúda do trabalhador, além da possibilidade de ocorrer possíveis erros de humanos voltados a identificação e medição das árvores. O uso de geotecnologia remotas através das aeronaves para levantamento e mapeamento da vegetação vem sendo um verdadeiro aliado aos gestores ambientais na execução de projetos de manejo e conservação florestal. Considerado o potencial de uso desta ferramenta, o objetivo deste estudo foi buscar avanços técnicos e científicos para apoiar o inventário florestal remoto na floresta Amazônica, apresentado em dois capítulos. O Capítulo I corresponde a fusão de imagens aéreas adquiridas por meio de um sistema de aeronave não tripulada visando a identificação automática de espécies arbóreas utilizando rede neural convulacional (CNN) na floresta Amazônica. O estudo foi realizado em uma área de floresta nativa com 260 ha em Rio Branco, na sede da Embrapa Acre, em que foram identificadas e segmentado oito espécies florestais com potencial econômico, totalizando 406 indivíduos, com DAP a partir de 50 cm. A classificação automática das espécies foi feita através da CNN ResNet-18 combinada com a arquitetura DeepLabv3+, modelo de aprendizado de máquina profundo, dividiu-se o banco de dados em 60% treinamento e 40% para teste. O melhor resultado foi na fusão das imagens aéreas de diferentes meses (período seco e chuvoso), a acurácia média foi de 90,5%, onde para seis espécies a acurácia ultrapassou 90%, a espécie *Phyllocarpus riedelii* obteve uma acurácia de 100%. O mês de maio teve a menor acurácia, 69,3%, intensa mudança de fenofases das espécies, mais difícil para o algorítmico discriminar as espécies florestais enquanto que o melhor mês foi o de novembro, acurácia de 83,5%. O capítulo II abordou sobre a estimativa do volume de árvores a partir da morfometria da copa obtidas por UAS na mesma área de estudo. Utilizou-se o inventário florestal de campo, onde todas as árvores com diâmetro a altura do peito - DAP $\geq$ 50 cm foram mensuradas. A localização das árvores foram combinadas com as imagens aéreas e, após, filtrados 388 indivíduos distribuídos em 55 espécies. A morfometria da copa foi identificada através do diâmetro médio e da área da copa, posteriormente realizou um teste de correlação para analisar o tamanho do relacionado destas variáveis para posterior inserção nos modelos de volume, área basal e diâmetro das árvores distribuído por classe diamétrica. O banco de dados foi dividido em 70% para o treinamento e 30% para o teste. O teste de correlação identificou uma forte interação entre as variáveis da copa com volume e a inexistência da altura, logo foi descartada da análise. O volume predito teve métricas para o ajuste SEE 21,97% e para o teste RMSE 19,13%, ambos com R^2 superior a 0,90. Para área basal e diâmetro o SEE foi inferior a 6,5% e R^2 maior que 0,99, os resíduos dos modelos foram heterocedáticos, o volume teve a maior dispersão, mas concentrou-se até $\pm$ 25% demonstrando a acurácia do modelo e o potencial em utilizar variáveis da copa das árvores.

Palavras-chave: 1. Imagens aéreas 2. Diâmetro 3. segmentação 4. ortomosaico 5. acurácia

ABSTRACT

Performing a forest inventory is an indispensable field survey method for knowing the quantitative and qualitative characteristics of a forest. This activity in native forests is time-consuming, costly, poses a risk to the worker's health, in addition to the possibility of possible human errors in identifying and measuring trees. The use of remote geotechnology through aircraft for surveying and mapping vegetation has been a true ally to environmental managers in executing forest management and conservation projects. Considering the potential use of this tool, the objective of this study was to seek technical and scientific advances to support the remote forest inventory in the Amazon rainforest, presented in two chapters. Chapter I corresponds to a fusion of aerial images acquired through an unmanned aircraft system aiming to automatically identify tree species using convulational neural network (CNN) in the Amazon rainforest. The study was conducted in an area of native forest with 260 ha in Rio Branco, Acre, Brazil, at the headquarters of Embrapa Acre, where eight forest species with economic potential were identified and segmented, totaling 406 individuals, with DBH from 50 cm. The automatic classification of species was done through CNN ResNet-18 combined with the DeepLabv3+ architecture, a deep machine learning model, and the database was divided into 60% training and 40% for testing. The best result was in the fusion of aerial images from different months (dry and rainy seasons); the average accuracy was 90.5%, it exceeded 90% for six species, and the *Phyllocarpus riedelii* species obtained an accuracy of 100%. The month of May had the lowest accuracy (69.3%), with intense change in the phenophases of the species, making it more difficult for the algorithm to discriminate forest species, while the best month was November, presenting an accuracy of 83.5%. Chapter II addressed the volume estimation of trees from crown morphometry obtained by UAS in the same study area. A field forest inventory was used, where all trees with diameter at breast height - DBH ≥ 50 cm were measured. The locations of the trees were combined with the aerial images, and then 388 individuals distributed in 55 species were filtered. The canopy morphometry was identified through the average diameter and the canopy area, and a correlation test was subsequently performed to analyze the related size of these variables to later insert the volume, basal area and diameter of the trees distributed by diametric class in the models. The database was divided into 70% for training and 30% for testing. The correlation test identified a strong interaction between the canopy variables with volume and the lack of height, which was therefore discarded from the analysis. The predicted volume had metrics of 21.97% for the SEE fit and 19.13% for the RMSE test, both with R^2 greater than 0.90. The SEE for basal area and diameter was less than 6.5% and R^2 greater than 0.99; the residuals of the models were heteroscedastic, the volume had the greatest dispersion, but was concentrated up to ± 25%, thereby demonstrating the model accuracy and the potential to use treetop variables.

Keywords: 1. Aerial images 2. Diameter 3. segmentation 4. orthomosaic 5. accuracy

LIST OF FIGURES

Chapter I

Chapter II

LIST OF TABLES

Chapter I

Chapter II

SUMMARY

GENERAL INTRODUCTION

The Amazon Forest is the largest tropical forest in the world, home to high biodiversity and a powerful stock of forest resources capable of sequestering carbon and contributing to global climate regulation (Heinrich et al., 2021). The conservation of its territory is being impacted by deforestation arising from invasions of public and private lands, converting it into pasture and agriculture. The expansion of consolidated private areas also contributes to the increase in CO_2 emissions.

The valuation of ecosystem services through the sustainable use of forest resources is a possible solution for protecting the forest, developing an economy based on exploiting existing raw materials, wood and non-wood products (Lima and Azevedo-Ramos, 2021).

The forest inventory is an indispensable tool for knowing the quantitative and qualitative characteristics of a forest, which is necessary to outline the viability of forest conservation and management projects. Field activities in native forests are time consuming, costly, and unhealthy for workers, identification and measurement errors may occur, and above all, have high costs. With the advance in the availability of high resolution aerial images and the use of active and passive sensors (i.e. LiDAR and RGB, respectively), it has become possible to remotely identify tree species in native forests, estimate biomass, and analyze ecological succession, thereby optimizing time, reducing financial resources and increasing area coverage capacity.

The use of passive and active sensors, such as LiDAR, has gained a lot of space in the forestry sector, as it is able to go beyond the treetops (something that the RGB sensor is not capable of) and collect relief information, individualize trees, estimate height, structure the understory, estimate biomass and consequently carbon (de Almeida et al., 2021; Ferreira et al., 2019; Leite et al. 2022). Figueiredo et al. (2014) evaluated the morphometry volume of the tree canopy in the Amazon using LiDAR data from plane, reaching estimates of 92.92% of R^2 and a mean error of 16.73% for equations with the DBH variable present and 79.44% of R^2 and 27.47% of Syx(%) for the equation without DBH, constituting an important work portraying the viability of carrying out a remote forest inventory.

The availability of high-resolution satellite images contributes to monitoring large areas of forests. Works aimed at identifying species have focused on the use of Sentinel-2 and WorldWiew images combined with machine learning (Lassalle et al., 2022; Ma et al., 2021). Ferreira et al. (2021) used convolutional neural networks (CNN) to identify individuals of the species *Berthollethia excelsa* Bonpl. through the canopy (Lecythidaceae) in the Amazon

rainforest from high resolution images from the WorldView-3 satellite (pixel size = 30 cm), and achieved an average accuracy greater than 93.0%, demonstrating the robustness of combining high resolution images with CNNs being able to discriminate the chestnut tree for large tracts of forest at a low cost.

The use of aircraft to map vegetation has been a true ally to environmental managers in executing forest management, inspection, monitoring and conservation projects (d'Oliveira et al., 2021; d'Oliveira et al., 2020; de Almeida Papa et al., 2020b; Figueiredo et al., 2016; da Costa et al., 2021; da Cunha Neto et al., 2021). Corte et al. (2022) estimated the height (ht), diameter (DBH) and volume (v) of a silvopastoral eucalyptus plantation using a UAS with LiDAR sensor, in which the erro for DBH was 9.33%, ht was 12.40% and volume 26.36%, claiming to be a valid alternative to support decision-making on forest management activities, especially when considering tree architecture and biomass components.

With the popularization of Unmanned Aircraft System (UAS) with an RGB sensor, a great advance has been taking place in remote data collection in plant and native forests (Mohan et al., 2017; Novak et al., 2020; Schiefer et al., 2020; Nasiri et al., 2021; Kuzmin et al., 2021; Hartley et al., 2020). The discrimination of native species is already a reality; for example, Ferreira et al. (2020b) applied CNN from aerial UAS images with RGB sensor (pixel = 4 cm) in an area of native forest in the Amazon (135 hectares) to classify the species *Attalea butyracea*, *Euterpe precatoria* and *Iriartea deltoidea*, obtaining positive results with a mean accuracy of 78.6%, 98.6% and 96.6%, respectively; and also enabling identification of palm trees in the Amazon, an important by-product of the forest responsible for the economy of several traditional families, and crucial for the improvement of non-timber forest management. Moura et al. (2021a) used UAS images combined with CNN to evaluate forest regeneration in the same region and managed to classify six forest species which are indicators of an environment in recovery with an average accuracy above 90%, demonstrating the potential of using aerial images to assess the quality regeneration of disturbed environments.

High-resolution images, especially from the LiDAR sensor on NASA's Global Ecosystem Dynamics Investigation (GEDI) satellite or a UAS, are so powerful that they can predict wildfire risks in fire-prone areas; this in turn allows for more detailed planning actions among public institutions to minimize possible impacts that fire may have on the forest, such as loss of biodiversity, carbon and alteration of microecosystems, in addition to social impacts, as reported by Leite et al. (2022), inferring about regions with potential for forest fire in tropical savannah.

Remote data collection in forests is gaining regional proportions; for example, in combining UAS with Satellite, it became possible to evaluate large areas with a low cost and reduced field effort, demonstrating the potential of this technology (Mohan et al., 2021; Parmehr and Amati, 2021; Lahssini et al., 2022; de Almeida et al., 2021; You et al., 2022).

The main hypothesis of this study is that the use of geotechnologies in native forests makes it possible to understand forest resources more quickly, and is able to subsidize a more precise and dynamic planning of environmental refuse in the Amazon. This hypothesis was tested by dividing the thesis into four parts: two chapters in article format, a general consideration and a general conclusion.

The first chapter corresponds to discriminating eight forest species of economic value in the Amazon from the use of CNN with aerial images of UAS and corresponds to an article published in the Ecological Informatics journal. It is important to emphasize that the inclusion of the article in this thesis is in accordance with the rights that the authors have when publishing with Elsevier. The second chapter deals with commercial volume estimates for trees based on crown morphometry from aerial images of UAS. Conducting a traditional forest inventory is essential to know the qualitative and quantitative characteristics of the native forest in the Amazon. However, the logistics are responsible for a large part of the costs, the sampling area is reduced and limited due to the access and adverse conditions of the forest; therefore, the use of a UAS with RGB sensor allows you to map hundreds of hectares compared to traditional field survey methods, as they are very widespread and easily accessible in the market, the manpower in the field is reduced and the risks to the health of the field worker are lower.

These two chapters seek to make a preliminary inventory of the existing commercial timber stock in the native forest feasible, from species classification to preliminary remote estimation of the commercial tree stock. General considerations are presented to indicate the links between the chapters of the thesis and comments on future work on the subject. Finally, the last part refers to the general conclusion found in this thesis.

OBJECTIVES

The general objective of this study was to enable a preliminary commercial remote forest inventory in a native forest area in the Amazon through the use of remotely piloted aircraft with an RGB sensor to capture aerial images. Thus, the specific objectives are outlined in two chapters:

I. Discriminate forest species through the use of deep machine learning from convolutional neural network for aerial images of different months.

II. Estimate the volume, basal area and diameter of commercial trees from crown parameters derived from aerial images.

CHAPTER 1

FUSING MULTI-SEASON UAS IMAGES WITH CONVOLUTIONAL NEURAL NETWORKS TO MAP TREE SPECIES IN AMAZON FORESTS

*Chapter formatted and published in the magazine Ecological Informatics. DOI: https://doi.org/10.1016/j.ecoinf.2022.101815

FUSING MULTI-SEASON UAS IMAGES WITH CONVOLUTIONAL NEURAL NETWORKS TO MAP TREE SPECIES IN AMAZON FORESTS

Hudson Franklin Pessoa Veras[a*], Matheus Pinheiro Ferreira[b], Ernandes Macedo da Cunha Neto[a], Evandro Orfanó Figueiredo[c], Ana Paula Dalla Corte[a], Carlos Roberto Sanquetta[a]

[a]*Departament of Forest Science, Federal University of Paran*a *(UFPR), Pref. Lothario Meissner Avenue 900, 80210-170 Curitiba, PR, Brazil*

[b]*Cartographic Engineering Department, Military Institute of Engineering (IME), Praça Gen. Tibúrcio 80, 22290-270 Rio de Janeiro, RJ, Brazil*

[c]*Embrapa Acre, Rodovia BR-364, km 14, 69900-056 Rio Branco, AC, Brazil*

ABSTRACT

Remote sensing images obtained by unoccupied aircraft systems (UAS) across different seasons enabled capturing of species-specific phenological patterns of tropical trees. The application of UAS multi-season images to classify tropical tree species is still poorly understood. In this study, we used RGB images from different seasons obtained by a low cost UAS and convolutional neural networks (CNNs) to map tree species in an Amazon forest. Individual tree crowns (ITC) were outlined in the UAS images and identified to the species level using forest inventory data. The CNN model was trained with images obtained in February, May, August, and November. The classification accuracy in the rainy season (November and February) was higher than in the dry season (May and August). Fusing images from multiple seasons improved the average accuracy of tree species classification by up to 21.1 percentage points, reaching 90.5%. The CNN model can learn species-specific phenological characteristics that impact the classification accuracy, such as leaf fall in the dry season, which highlights its potential to discriminate species in various conditions. We produced high-quality individual tree crown maps of the species using a post-processing procedure. The combination of multi-season UAS images and CNNs has the potential to map tree species in the Amazon, providing valuable insights for forest management and conservation initiatives.

Keywords: Individual tree crowns Deep learning Multi-temporal images Phenology Tropical forest

1. Introduction

Information regarding characteristics of tropical forests, such as aboveground biomass and tree species composition, is crucial for their sustainable management. Forest inventories are the most common approach used to retrieve such characteristics. However, due to prohibitive costs, they are usually limited to small spatial extents (< 1% of the sampling area). The combination of remote sensing and forest inventory data has provided accurate information on forest characteristics over large areas (hundreds of hectares) and proved helpful in reducing field effort (Dalla Corte et al., 2020; de Almeida Papa et al., 2020).

Remote sensing images acquired by UAS platforms have been employed to retrieve characteristics of tropical forests, particularly the spatial distribution of tree species. UAS-based data acquisition usually results in hundreds of ultra-high spatial resolution (ground sampling distance, GSD < 10 cm) RGB images, which enable retrieving fine-scale features of individual tree crowns, such as the arrangement of leaves and branches. Previous investigations showed that deep learning methods can automatically learn these features on ultra-high resolution images acquired by UAS and successfully discriminate species (Ferreira et al., 2020; Kattenborn et al., 2021; Morales et al., 2018).

The most common deep learning method is convolutional neural networks (CNNs). CNNs rely on convolutions (local linear operations) to automatically extract object features (e.g., shapes, edges, texture) without user intervention (Zhang et al., 2016). CNNs were initially designed to perform scene classification, that is, classifying the image as a whole into one of several different classes. CNNs for object detection can locate the object within the image by constructing a bounding box that encloses it. Semantic segmentation networks aim to assign a label to each image pixel, while instance segmentation networks combine object detection and semantic segmentation to precisely outline the object's contour. Semantic and instance segmentation methods can simultaneously classify and detect ITCs, making them an alternative to object-based approaches that require an image segmentation step before classification (Blaschke, 2010).

Image segmentation algorithms are computationally intensive and require empirical parameter tuning. Moreover, applying these algorithms to delineate ITCs in tropical forests usually does not produce reliable results because of the structural complexity of the canopy (Tochon et al., 2015; Wagner et al., 2018). Although ITC delineation provides valuable insights for forest management, such as crown size and shape, retrieving the exact contour of ITCs to map tree species is not essential. ITC delineation can be performed using instance segmentation

approaches such as Mask R-CNN (He et al., 2017) or improved YOLO variants (e.g., (Hurtik et al., 2022)). However, these methods have prohibitive computational costs because they are composed of two deep neural networks, one to detect the objects and another to label the pixels that belong to them. In turn, semantic segmentation networks provide a more straightforward and fast way to map tree species at the ITC level (Ferreira et al., 2020). Recent works, motivated by the great flexibility in data acquisition provided by UAS, used remote sensing images from multiple seasons to map tree species. Most studies were performed in temperate forests (e.g., Natesan et al., 2020; Grybas and Congalton, 2021; Belcore et al., 2021; Liu, 2022) in which seasons are well defined and tree species diversity is limited. In tropical forests, tree species usually have complex phenological patterns, and selecting the most relevant time frame for image acquisition to map a set of tree species is challenging. Images acquired by RGB sensors onboard UAS enable capturing and quantifying fine-scale features of ITCs. CNNs can automatically learn species-specific features in ultra-high spatial resolution RGB images.

Previous studies showed the capacity of CNNs to differentiate among palm species in Amazon forests by detecting crown architectural patterns (e.g., Ferreira et al., 2020; Morales et al., 2018). To improve tree species mapping, it is worth exploring other features, such as seasonal variations in plant characteristics caused by phenology. In this regard, multi-season images can be used to track phenological events such as flowering, fruiting, and leaf falling. The combined use of CNNs with multi-season UAS images has been poorly investigated, particularly in humid tropical forests where trees show highly diverse phenological patterns.

This study examines the utility of using multi-season RGB images acquired by low cost UAS and CNNs to map tree species at the ITC level in Brazilian Amazon forests. We tested the following hypothesis: CNNs can learn species-specific phenological characteristics; thus, fusing multi-season images for model training improves classification accuracy. To test our hypothesis, we defined two fundamental objectives (i) acquire UAS images along the year, encompassing the two main seasons in Amazonia; (ii) assess the classification accuracy of a CNN model trained with single-date and multi-date images.

2. Materials

2.1. Study area

The study area is an experimental forest of the Brazilian Agricultural Research Company (Embrapa) located in the municipality of Rio Branco, Acre state, Brazil (10∘01′22”S,

67∘40′3”W) (Fig. 1a). It is a highly diverse native rainforest area of 1600 ha about 200 m above the sea level (a.s.l).

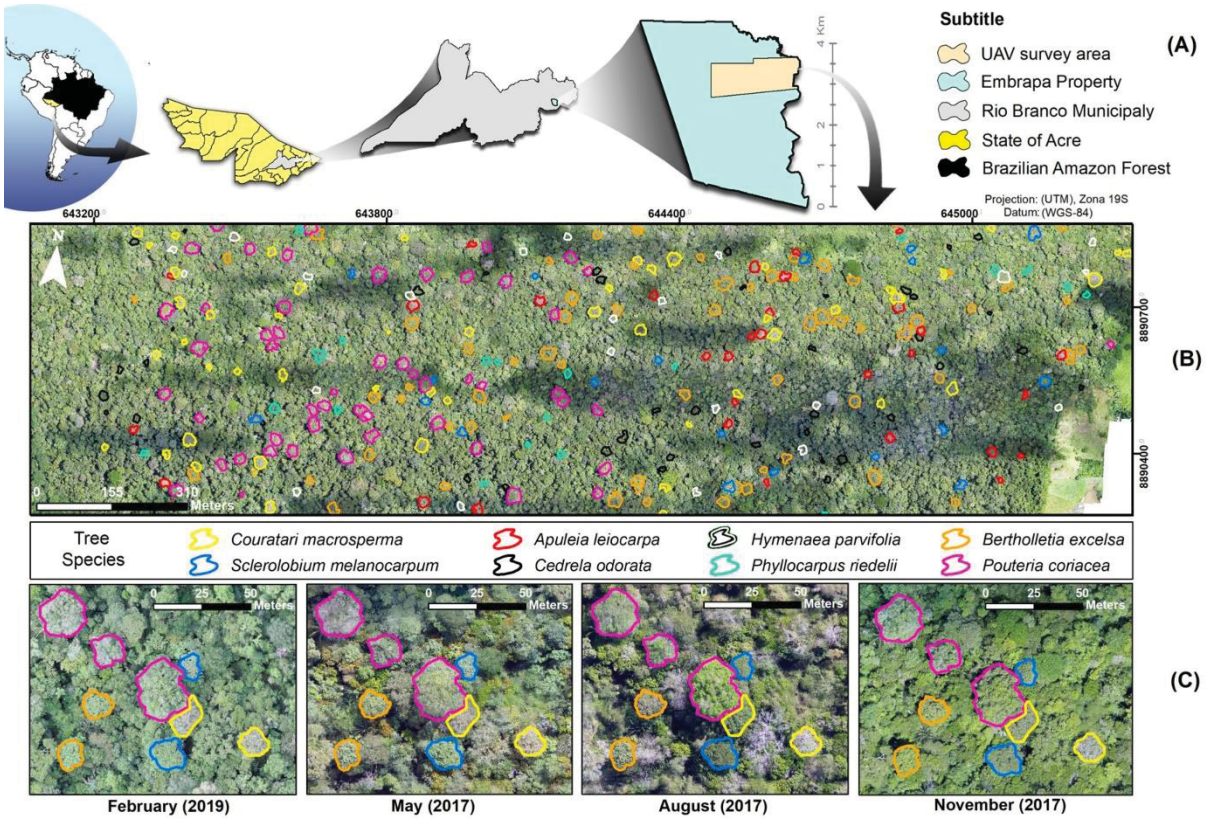

Fig. 1. (A) Location of the study area in the Acre state, southwestern Amazon, Brazil. (B) True color (RGB) composition of the orthomosaic with manually delineated individual tree crowns (ITCs) overlaid. (C) Examples of UAS images acquired in February, May, August, and November.

The orthomosaic used in this study comprises 260 ha. The experimental forest area receives 1950 mm of rain annually, and the average temperature is 24.8 (±0.8)ºC (Ramos et al., 2009). The vegetation of the area is classified as an open rainforest with the presence of palms and bamboos (ACRE, 2010).

2.2. UAS images

We collected aerial images with the UAS DJI Phantom 4 Pro, equipped with an RGB (red, green, blue) CMOS sensor of 20-megapixel resolution, a 24 mm autofocus lens, and a manual shutter with autonomy up to 30 min. The UAS flew 120 m above the forest canopy with a cruising speed of 10 m/s, resulting in images with a GSD (Ground Sample Distance) of 4 cm.

UAS mapping was always performed between 10:00 and 14:00, the time of greatest sunlight availability on the Forest during the study months. We took a total of 1,585 images with a forward overlap of 86.0% and side lap of 86.36% in eight consecutive flights. Ten sequential flights were carried out to map the entire study area in different months and no treatment was performed on the images in order to portray the field condition and minimize processes. We established three ground control points (GCPs) on the edges of the forest reserve before the flights. A dual-frequency GNSS receiver was installed at each GCP and collected GPS and GLONASS data for 241 min. The average horizontal and vertical precision of the GCPs after post-processing were 10 cm and 3 cm, respectively. Finally, we used the PiX4D software program (Pix4D Inc.) to generate orthomosaics of the study area.

We acquired UAS images in different months to capture species-specific phenological characteristics such as leaf fall, flowering, changes in leaf color, and fruiting patterns. The aim was to encompass two main seasons in Amazonia: the dry and wet seasons. Thus, we used images from February (peak of the wet season), May (end of the wet season), August (peak of the dry season), and November (end of the dry season). Examples of multi-season UAS images are shown in Fig. 1c.

3. Methods

3.1. Individual tree crown (ITC) dataset

In the experimental forest area, we measured and identified to the species level all trees with a diameter at breast height (DBH) >50 cm. The traditional forest inventory was conducted throughout the Native Forest of Embrapa Acre, however we extracted a portion to be combined with the mapping carried out by the UAS. For this study, we selected the most economically important species for nut and timber production and delineated their ITCs in the UAS images (GSD = 4 cm). We identified each ITC to the species level using information from the forest inventory georeferencing and expert knowledge from botanical identification. Manual ITC delineation was carefully performed so that a single ITC polygon encompasses the same tree in all four images (Fig. 1c). We outlined a total of 406 ITCs, corresponding to eight species. The number of ITCs per species, as well as the number of pixels, are shown in Table 1.

Table 1. List of tree species with crowns manually delineated in the UAS orthomosaic and identified to the species level: species names, number of individual tree crowns (ITCs) and average number of pixels per ITC.

Scientific name	Popular name	No of ITCs	No of pixels	Average no of pixels per ITC	Average crown diameter (pixels)
Pouteria coriacea (Pierre) Pierre	Abiorana-rosa	74	16,371,007	221,230	616
Bertholletia excelsa Bonpl.	Castanheira	85	15,653,626	184,160	550
Cedrela odorata L.	Cedro	52	3,906,764	75,130	359
Apuleia leiocarpa (Vogel) J.F. Macbr.	Garapeira	45	5,210,028	115,778	446
Phyllocarpus riedelii Tul.	Guaribeiro	24	2,014,050	83,919	398
Hymenaea parvifolia Huber	Jutaí	32	3,685,441	115,170	443
Sclerolobium melanocarpu Ducke	Tachi	27	3,352,427	115,170	432
Couratari macrosperma A. C. Sm.	Tauari	67	9,967,430	124,164	505

3.1.1. Tree species classification method

We performed tree species classification using the ResNet-18 (He et al., 2016) CNN incorporated into the DeepLabv3+ architecture (Chen et al., 2018), which is considered a state-of-the-art deep learning model for semantic segmentation and was successfully used for tree species classification from remotely sensed images (Morales et al., 2018; Ferreira et al., 2021, 2020). We used ResNet-18 because it has the best trade-off between computational time and classification accuracy compared to other ResNet variants in preliminary tests. The ResNet-18 comprises residual blocks that forward the feature maps (activations) from shallow to deeper layers using the so-called skip connections, which allows the training of much deeper models. DeepLabv3+ is an encoder-decoder architecture designed to capture multi-level features. The encoder module performs feature extraction by gradually reducing the spatial dimension of the input image. The decoder recovers the original size of the input image and performs semantic segmentation using features extracted by the encoder. (Fig. 2). More details regarding ResNet-18 and DeepLabv3+ can be found in He et al. (2016) and Chen et al. (2018), respectively.

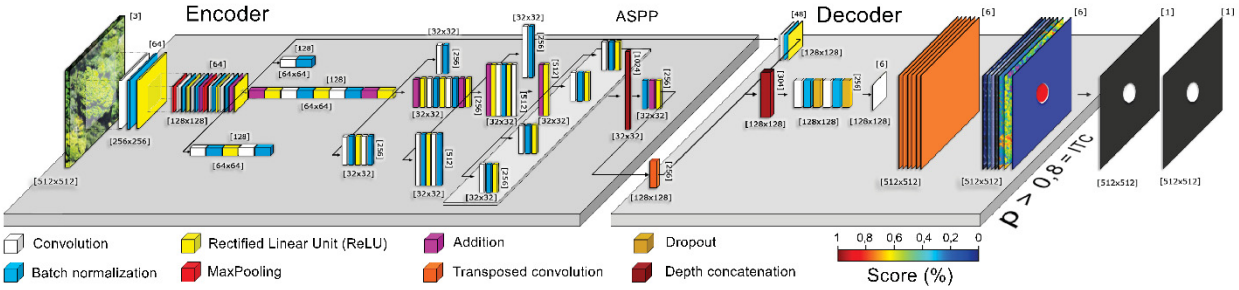

Fig. 2. DeepLabv3+ architecture with the ResNet-18 backbone network. The encoder module uses convolution operations and activation functions (ReLU) to extract features of tree species. The spatial dimension of the image is reduced by a factor of 16 at the end of the convolution process. The decoder module recovers the spatial dimension using transposed convolution operations. The softmax classifier is applied to generate score maps for each class. Finally, a probability rule is applied to detect the ITCs of target tree species within the input image patch.

Semantic segmentation networks are usually trained with densely labeled datasets, in which all pixels from a training image patch are labeled, meaning that they belong to a given class. This further means that it is expected that all classes present in the image patch should be known beforehand. In the case of map tree species in tropical forests, and given the highly diverse nature of these ecosystems, knowing all the tree species contained in an image patch is very unlikely. Thus, we trained our model using only the pixels from the target tree species (Table 1). To do this, we used a modified cost function that propagates the errors of desired classes only, as proposed by Martins et al. (2021).

3.1.2. Post-processing procedures

A semantic segmentation model will classify all pixels from an input image patch according to the number of classes used to train the model. In our case, the image pixels are labeled into eight species. However, the study area contains >200 tree species (Section 2.1), and labeling all of them as one of the eight target species represents an oversimplification. To avoid labeling all image pixels, we decided to classify them based on class membership probabilities, which indicate the confidence level of the predictions. A pixel is labeled in the scores maps of each species if its probability of belonging to that species is higher than 0.8, as this probability value is widely practiced by similar works (Ferreira et al. 2020; Martins et al. 2021), and is therefore used in this study. Otherwise, the pixel is considered an unknown

species. We verified that this procedure produced realistic species maps in which ITCs of the target species are detected.

3.2. Experimental set-up

First, we separated the ITCs into 60% for training and 40% for testing. Then, we performed a vector-to-raster conversion of the ITC polygons to produce a densely labeled dataset containing class information of each image pixel. Notably, pixels from non-target species were not considered during network training (see Section 3.1.1).

We produced a synthetic image using the training ITCs. We randomly chose five pixels for each ITC, from which we grew patches of size 1024 × 1024 pixels. We then extracted these patches from the UAS and the labeled image and concatenated them into one rectangular tiled image (Fig. 3). Finally, we randomly extracted 2500 patches of size 512 × 512 pixels from the synthetic image to feed the network with training data. We extracted a new set of 2500 patches for each epoch. We used the stochastic gradient descent with momentum (SGDM) algorithm to update the network parameters (weights and biases) (Murphy, 2012). The total number of epochs was 25, as the classification accuracy did not change significantly after this number of epochs. The mini-batch size was 12, according to the available memory in the GPU. We used random reflection and rotation operations to augment the training data and to prevent the network from overfitting.

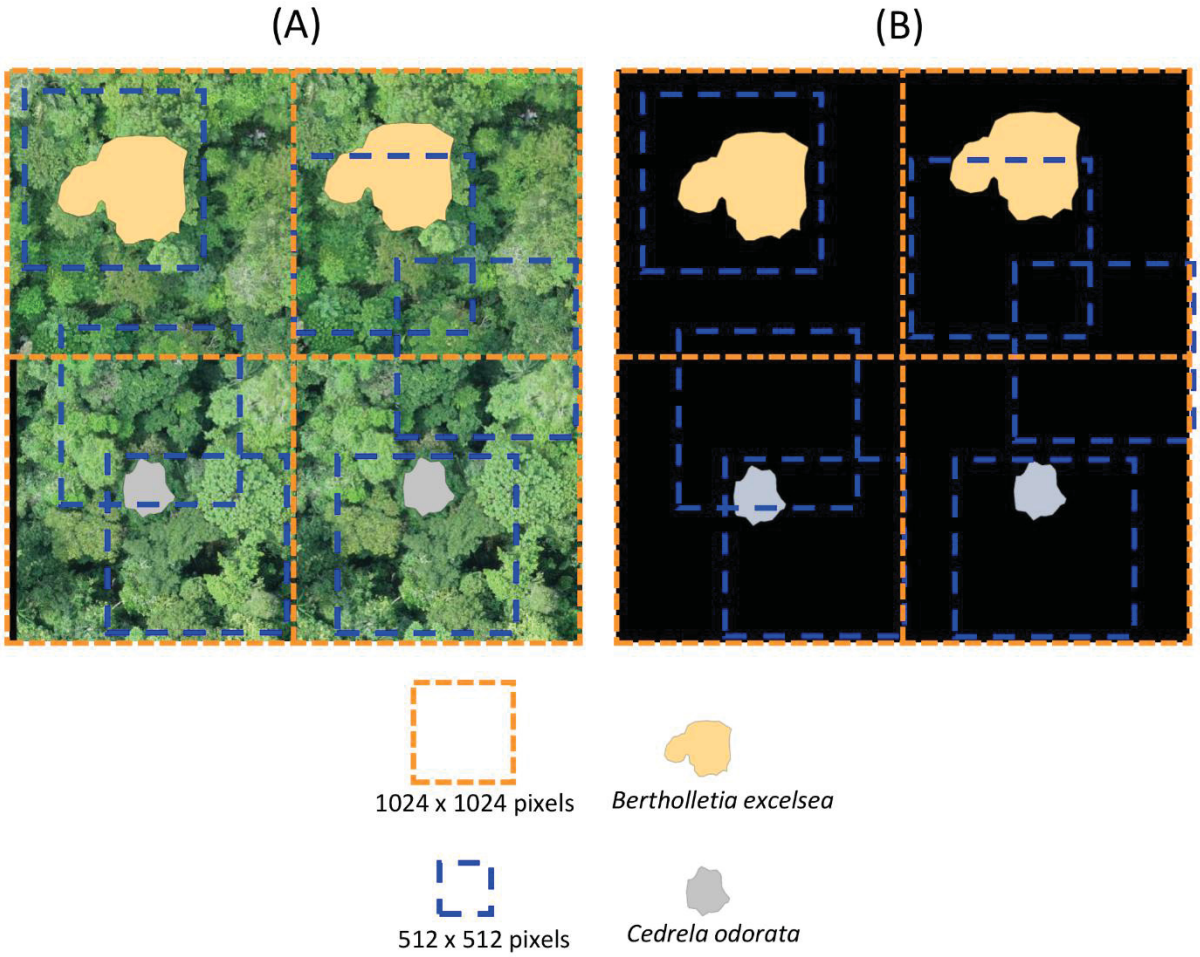

Fig. 3. Illustration of the model training strategy. (A) Synthetic image created from the original orthomosaic. (B) Labeled image. Image patches of size 1024 × 1024 (orange dotted squares) are created from randomly selected pixels of individual tree crowns of the target species (Table 1). These patches are concatenated into one rectangular tiled image. Then, patches of 512 × 512 (blue dotted squares) are randomly extracted from the synthetic and labeled image to feed the network with training data. (For interpretation of the references to color in this figure legend, the reader is referred to the web version of this article.)

We performed two experiments to evaluate the use of multi-temporal images to discriminate among the species: (i) we used the images from each month (February, May, August, and November) individually, and (ii) we combined the images from each month into a single 12-bands image to train our model. This process is called early fusion, and is capable of merging all image bands at the beginning of processing. The data are aligned and merged without any pre-processing, thus being suitable for exploring cross-correlations between reference data, increasing the system performance. Training and inference were performed on a desktop workstation with an Intel Core i7–8700 3.2GHz CPU, 64GB of main memory, and

an NVIDIA® GeForce Titan V GPU with 12GB of dedicated memory and 5120 CUDA® cores. All image processing procedures were implemented on the Matlab® enviroment. The average computational time spent on the entire image processing routine and CNN output was seven hours.

3.3. Accuracy assessment

The accuracy assessment was performed with the testing ITCs, which were not used for training. We computed the confusion matrices with intersecting samples between the reference and predicted ITCs. From the confusion matrices, we calculated the user's and producer's accuracy, the F1-score. The user's accuracy (UA), also known as precision, is the probability that a pixel classified as a particular species represents that species in the reference:

$$UAi = \frac{TP_i}{TP_i + \sum_j M_{i,j}} \quad (1)$$

Where *TPii* is the percentage of true positives of species (i), and *Mij* is the number of pixels that truly belong to species (i) but were classified as class (j). The producer's accuracy (PA), also known as recall, is the probability that the pixels of a particular species are correctly classified in the reference, or:

$$PAi = \frac{TPi}{TPi + \sum_j M_{ij,}} \quad (2)$$

The F1-score is the harmonic mean between the user's and producer's accuracies, representing their balance. F1-score is computed as:

$$2\,\frac{(UA * PA)}{(UA + PA)} \quad (3)$$

Since we are not interested in outlining the ITC boundaries perfectly, we did not compute accuracy metrics designed for object detection, such as the intersection over union (IoU). Instead of IoU, we computed the percentage of ITCs correctly predicted in the test set. An ITC was considered correctly predicted if >50% of its pixels were correctly labeled by the model.

4. Results

The classification accuracy of tree species is shown in Fig. 4. The highest average accuracy was 90.5%, using images from all seasons. Combining images acquired in different seasons generally resulted in a significant decrease in the misclassification rate between species. For example, the misclassification between *P. riedelii* and *A. leiocarpa* was 49.1% in May and 0% in the multi-season composition. Similarly, *H. parvifolia* and *B. excelsa* showed misclassification rates above 35% in February and May but only 0.1% in the multi-season scenario. Such decreases in misclassification between species suggest that the network automatically learned how to select the most discriminative characteristics of each species in the multi-season images.

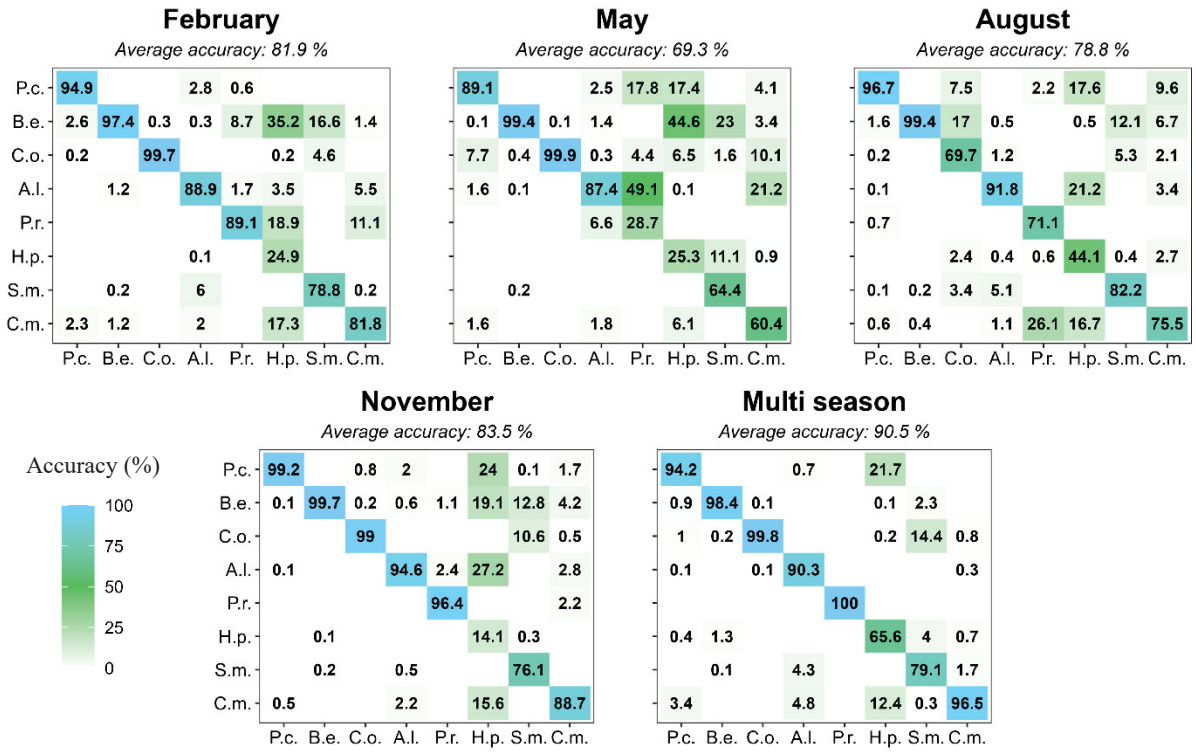

Fig. 4. Confusion matrices with the classification accuracy of tree species mapping using UAS images acquired in February, May, August, and November and a multi-season composition obtained by combining the images from each month. The producer's accuracy of each species in the diagonal cells (highlighted in blue), while the misclassification rate between species is shown in the off-diagonal cells. P.c. (*Pouteria coriacea*), B. e. (*Bertholletia excelsa*), C.o. (*Cedrela odorata*), A.p. (*Apuleia leiocarpa*), P.r. (*Phyllocarpus riedelii*), H.p. (*Hymenaea parvifolia*), S.m. (*Sclerolobium melanocarpum*), C.m. (*Couratari macrosperma*). (For interpretation of the references to color in this figure legend, the reader is referred to the web version of this article.)

The highest average accuracies were observed in the rainy season, meaning February and November, with 81.9% and 83.5%, respectively (Fig. 4). The average accuracy did not reach 80% in the dry season (May and August). Some species showed remarkable changes in the producer's accuracy between seasons. For example, the producer's accuracy of *C. odorata* was 99.7% in February and dropped to 69.7% in August (Fig. 4). Similarly, *P. riedelii* was classified with 96.4% accuracy in November and with 28.7% in May. The drops in the producer's accuracy of these species can be explained by leaf fall in the dry season. Fig. 5 shows an ITC of *C. odorata* in UAS images acquired in August (Fig. 5A) and November (Fig. 5B). One can note that the absence of leaves significantly changes the crown structure by exposing primary and lateral branches. Conversely, the fully foliated crown in the rainy season forms a billowy pattern. UAS images acquired in August and May show differences caused by leaf fall in an ITC of *P. riedelii* (Fig. 5C,D). Unlike, *C. odorata*, in August, the crown of *P. riedelii* does have leaves.

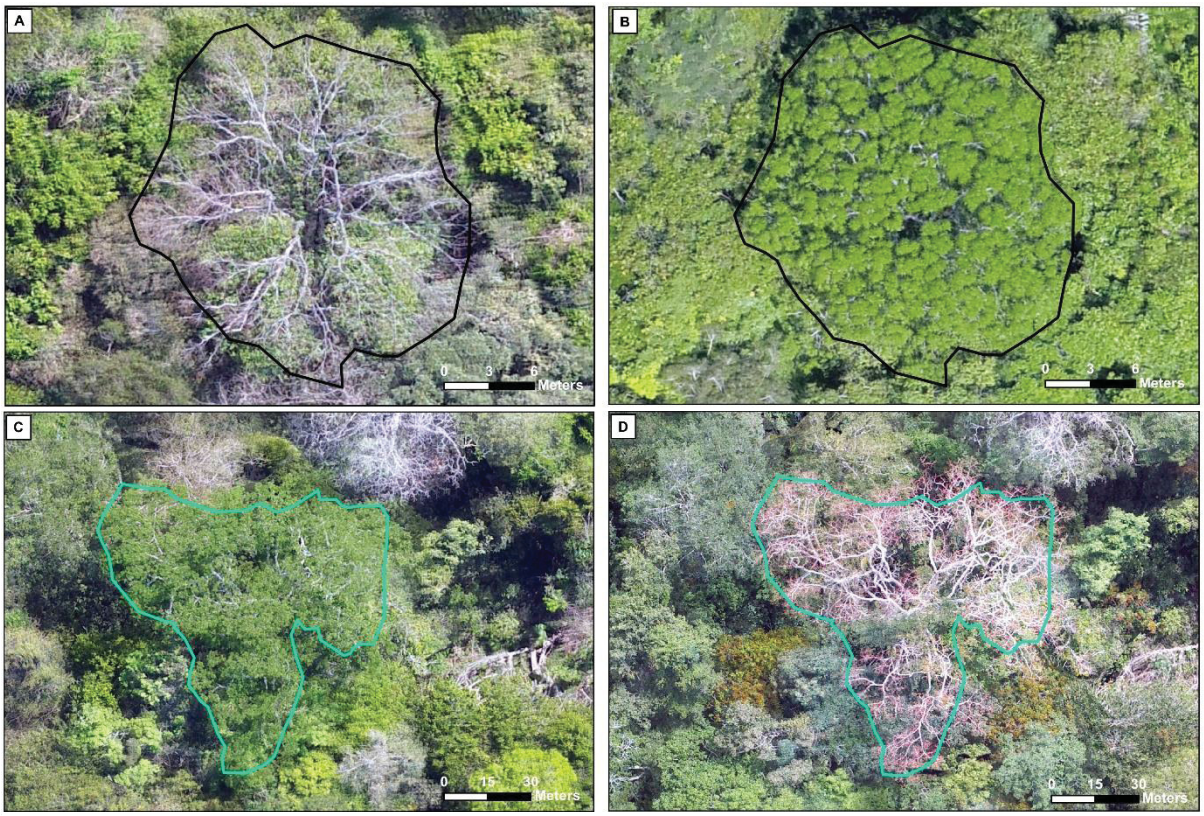

Fig. 5. UAS images of an individual tree crown of C. odorata obtained in August (A) and November (B) and P. riedelii in August (C) and May (D).

The combination of images from different months increased both the average classification accuracy (Fig. 4) and the F1-score of the species (Table 2). For example, the F1-

score of *H. parifolia* in November, February and May did not exceed 40% but increased to 65.1% after combining multi-season images. Using images from multiple seasons also increased the percentage of correctly predicted ITCs per species (Table 2). On average, more ITCs were correctly predicted in the rainy months (February and November) than in the dry seasons (May and August). Most of the tree species had >60% of their ITCs correctly predicted in the test set, except *P. riedelii*.

Table 2. User's accuracy (UA), producer's accuracy (PA), F1-score (F1), and percentage of individual tree crowns (ITCs) that were correctly predicted in the test set. The accuracy metrics result from classifications of UAS images acquired in February, May, August, and November and a multi-season composition of the images of all seasons.

Period	Accuracy	Species								Avarege
		P.c.	B.e.	C.o.	A.l.	P.r.	H.p.	S.m.	C.m.	
February	UA (%)	99.1	93.7	98.1	83.4	60.0	98.8	83.2	86.2	87.8
	PA(%)	94.9	97.4	99.7	88.9	89.1	24.9	78.8	81.8	81.9
	F1 (%)	96.9	95.5	98.9	86.0	71.7	39.8	80.9	84.0	81.7
	ITCs (%)	90.0	100.0	95.0	94.0	80.0	69.0	82.0	85.0	86.9
May	UA (%)	96.0	93.6	76.3	66.6	32.1	41.0	97.9	91.4	74.4
	PA(%)	89.1	99.4	99.9	87.4	28.7	25.3	64.4	60.4	69.3
	F1 (%)	92.4	96.4	86.5	75.6	30.3	31.3	77.7	72.7	70.4
	ITCs (%)	93.0	85.0	86.0	83.0	50.0	62.0	82.0	89.0	78.8
August	UA (%)	94.2	95.8	64.5	82.4	78.9	86.8	83.3	82.3	83.5
	PA(%)	96.7	99.4	69.7	91.8	71.1	44.1	82.2	75.5	78.8
	F1 (%)	95.4	97.5	67.0	86.9	74.8	58.5	82.7	78.8	80.2
	ITCs (%)	93.0	94.0	67.0	83.0	70.0	85.0	73.0	89.0	81.8
November	UA (%)	95.8	95.9	91.7	84.4	91.4	84.3	96.7	95.8	92.0
	PA(%)	99.2	99.7	99.0	94.6	96.4	14.1	76.1	88.7	83.5
	F1 (%)	97.5	97.8	95.2	89.2	93.8	24.2	85.1	92.1	84.4
	ITCs (%)	93.0	94.0	71.0	100.0	80.0	85.0	100.0	96.0	89.9
Multi-season	UA (%)	98.2	99.0	89.6	99.0	100.0	64.5	77.8	88.4	89.6
	PA(%)	94.2	98.4	99.8	90.3	100.0	65.6	79.1	96.5	90.5
	F1 (%)	96.1	98.7	94.4	94.4	100.0	65.1	78.4	92.3	89.9
	ITCs (%)	100.0	97.0	95.0	100.0	60.0	85.0	100.0	81.0	89.8

Examples of predictions obtained for images of each month are shown in Fig. 6. *P. coriacea*, *B. excelsa* and *A. leiocarpa* presented the homogeneous morphological characteristics during the year. The neural network model detected them in all months. Conversely, *C. odorata* showed a strong leaf fall in the dry season and was not detected by the model using the August image only (Fig. 6c). By combining images from multiple seasons *C. odorata* was successfully detected (Fig. 6e). In general, one can note a reduction in misclassification after using images from multiple seasons.

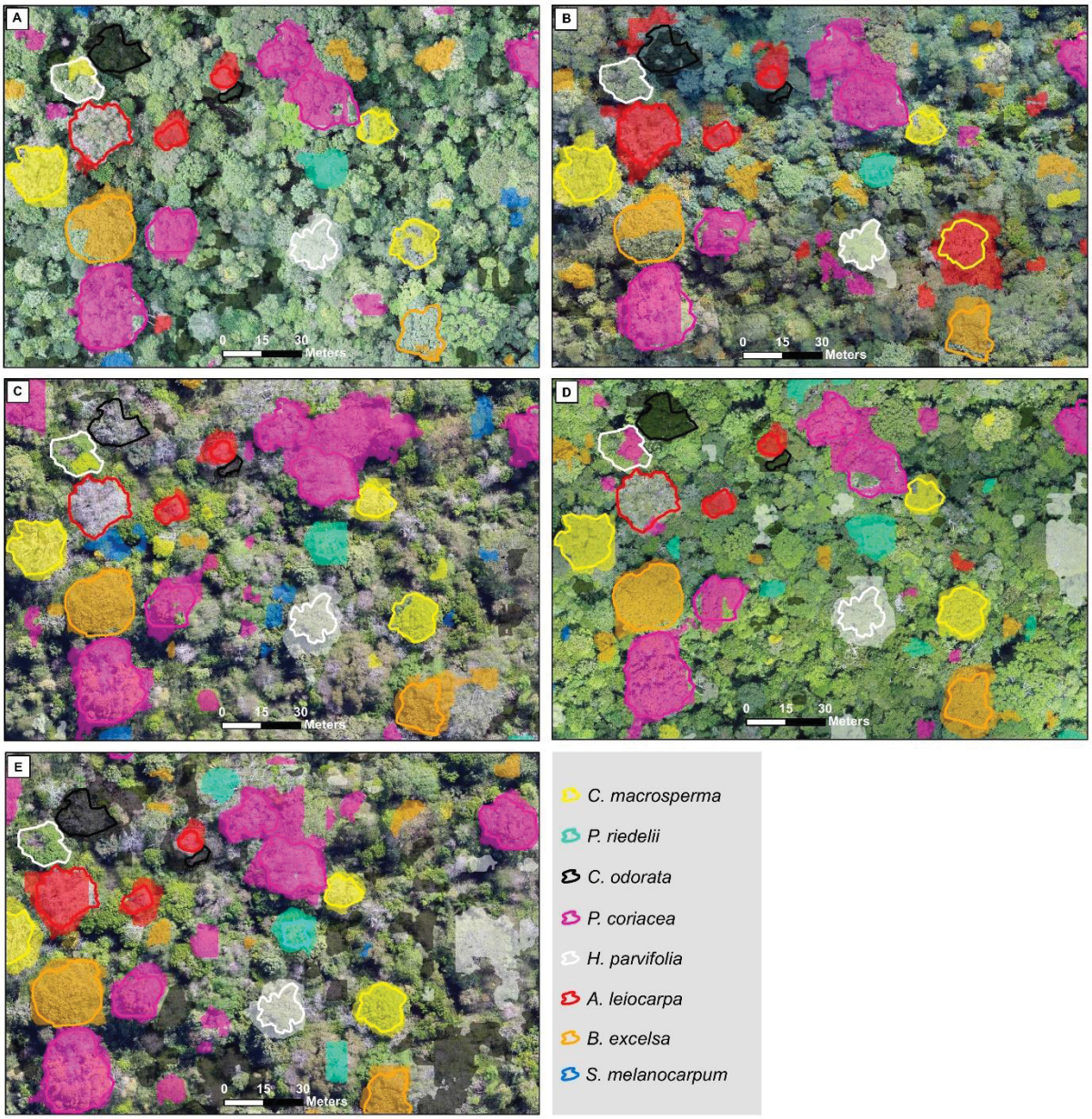

Fig. 6. Model predictions were obtained using images from (a) February, (b) May, (c) August, (d) November, and (e) a combination of all months. Reference ITCs not used to train the model

are shown as unfilled polygons, while model predictions are shown as filled polygons. For clarity, the UAS image shown in (e) is from August.

5. Discussion

Tree species mapping in Amazon forests using UAS images and CNNs is a powerful tool for forest conservation and management. User's accuracy in November ranged from 84.4% to 95.9%. Even species with <30 ITCs (*P. riedelii* and *S. melanocarpu*) reached high levels of classification accuracy, with F1-scores of 93.8% and 85.1%, respectively. *H. parvifolia* was the most challenging species to classify. Its ITCs showed highly variable patterns with several leafless trees, as well as a high degree of overlap between neighboring crowns. More ITCs of *H. parvifolia* are needed to incorporate its canopy structural variability in model training.

Nuijten et al. (2019) examined the multi-seasonal consistency of ITC segmentation in a Canadian forest and found that the beginning of leaf fall is an adequate period to segment ITCs because the canopy is less dense. The authors argue that when leaves begin to fall, the border among ITCs is more evident. Similarly, we observed an improvement in the visualization of *H. parvifolia* ITCs when their leaves started to fall in August. However, the beginning of leaf fall varied among the species. For example, in August, all *C. odorata* trees have already lost all their leaves, which negatively impacted the classification accuracy. Thus, we believe that the total absence of leaves hampers species detection.

The low cost of acquiring RGB images with a UAS and the flexibility of data acquisition promotes a more frequent use of multi-season images for tree species mapping. Natesan et al. (2020) used an RGB camera onboard a UAS to classify pine species in Canada over three years. The combination of annual images improved the classification accuracy, which reached 90% in some cases. Modzelewska et al. (2021) used hyperspectral data acquired in July (early summer), August (late summer), and October (autumn) acquired over a forest area in Poland to discriminate among seven tree species. The classification results show that a multi-season dataset produced the best results reaching 84–94% of overall accuracy.

In a temperate forest area in New Hampshire, USA, Grybas and Congalton (2021) investigated whether the classification accuracy of 14 tree species could be improved with multi-temporal UAS data. The authors collected five RGB images between April and June, encompassing the spring and summer seasons. They showed that a five-date stack of the multi-temporal images provided the best results (61.1% of overall accuracy). Studies using multi-

season RGB images acquired by UAS, particularly on the Brazilian Amazon, do not exist, thereby highlighting the relevance of this study.

To the best of our knowledge, this is the first study to show the potential of multi-season UAS images for classifying tree species in tropical forests. Another innovative aspect of our work is the classification method used. Most studies employed pixel-or object-based approaches along with classical machine learning algorithms such as random forests and support vector machines. In pixel-based approaches, pixels are usually labeled based on their spectral characteristics, thus neglecting the spatial relationship among neighboring pixels. Object-based procedures use a segmentation algorithm to delineate tree crows before classifying them. Image segmentation is challenging because it depends on empirical parameter settings and is computationally intensive, mainly if applied in UAS images featuring hyperspatial resolutions (GSD < 10 cm). The CNN models vanquish the limitations of both pixel-based and object-based approaches by simultaneously performing ITC delineation and classification. Moreover, CNN-based methods are robust to differences in viewing and illumination conditions (Natesan et al., 2020) and our results suggest that they learn species-specific phenological patterns.

Combining UAS images and deep learning for mapping tree species in Amazon forests paves the way for a new era in conservation and forest resource management (Onishi and Ise, 2021). The use of UAS for mapping native forests in the Amazon contributes to more optimized planning of environmental activities, helps to reduce costs and fieldwork, enabling access to the qualitative, quantitative, and spatial explicit characteristics of the forest in a faster and more dynamic way. Data collection flexibility provided by UAS particularly enabled taking advantage of multi-season images for tree species mapping.

This tool can be applied in areas intended for non-timber projects (açaí, brazilian chestnut, copaíba, palm trees in general) and timber (cedro, ipê, samaúma, abionara and others), verifying the potential of the forest at a low cost of field effort combined with high performance, along with less risk to the health of traditional workers, providing faster and more accurate information for the environmental manager’s decision-making, saving resources that would be applied in the field forest inventory activity, and assuming the risk of the area not being suitable for project execution.

Future work will focus on increasing the availability of images of native species through UAS mapping in different forests to contemplate a larger group of tree identification in the Amazon until it is possible to carry out forest inventories of large trees remotely.

6. Conclusions

In this work, we show that fusing RGB images from multiple seasons with CNNs improves tree species mapping in Amazon forests. By fusing images acquired in the rainy (November and February) and dry seasons (May and August), we verified an improvement in the classification accuracy of 27.2 percentage points compared with single-date classifications. We developed an effective model training strategy in which a synthetic image is produced based only on the reference ITCs. The use of CNNs and multi-season UAS images proved helpful in mapping economic relevant tree species in the Amazon and has the potential to contribute to forest management and conservation. Future studies will focus on expanding the ITC database by including more species. Moreover, we intend to analyze the generalization capability of our models to map tree species in other areas using low cost RGB images.

Acknowledgments

We gratefully acknowledge the support of NVIDIA Corporation with the donation of the Titan V GPU used for this research. M.P. Ferreira was supported by the Brazilian National Council for Scientific and Technological Development (CNPq) (grant 306345/2020-0) and the Carlos Chagas Filho Foundation for Research Support of the State of Rio de Janeiro (FAPERJ) grants #248496/2019 and #259727/2021. This study was funded in part by the Coordination for the Improvement of Higher Level Personnel (CAPES) - Finance Code 001 (A. Corte 88887.373249/2019-00), MC-371 TIC/CNPq No 28/2018 (408785/ 2018-7; 438875/2018-4), CNPq No 09/2018 (302891/2018-8).

References

Acre. Governo do Estado do Acre. Zoneamento Ecológico-Econômico do Estado do Acre, Fase II (Escala 1:250.000): Documento Síntese. 2. Ed. Rio Branco: SEMA, 2010. 356p. 1. ACRE – Zoneamento Ecológico-Econômico, 2. Meio Ambiente – Socioeconomia – Cultural/Político, 3. Gestão Territorial – Acre, I. Título.

de Almeida Papa, D., de Almeida, D.R.A., Silva, C.A., Figueiredo, E.O., Stark, S.C., Valbuena, R., Rodriguez, L.C.E., d'Oliveira, M.V.N., 2020. Evaluating tropical forest classification and field sampling stratification from LiDAR to reduce effort and enable landscape monitoring. For. Ecol. Manag. 457, 117634. URL: https://www.sciencedi

rect.com/science/article/pii/S037811271931179X. https://doi.org/10.1016/j.foreco.2019.117634.

Belcore, E., Pittarello, M., Lingua, A.M., Lonati, M., 2021. Mapping riparian habitats of natura 2000 network (91e0*, 3240) at individual tree level using UAS multi-temporal and multi-spectral data. Remote Sens. 13, 1756. Blaschke, T., 2010.

Object based image analysis for remote sensing. ISPRS J. Photogramm. Remote Sens. 65, 2–16. Chen, L.C., Zhu, Y., Papandreou, G., Schroff, F., Adam, H., 2018. Encoder-decoder with atrous separable convolution for semantic image segmentation. In: Proceedings of the European Conference on Computer Vision (ECCV), pp. 801–818.

Dalla Corte, A.P., Rex, F.E., Almeida, D.R.A.D., Sanquetta, C.R., Silva, C.A., Moura, M.M., Wilkinson, B., Zambrano, A.M.A., Cunha Neto, E.M.D., Veras, H.F.P., Moraes, A.D., Klauberg, C., Mohan, M., Cardil, A., Broadbent, E.N., 2020. Measuring individual tree diameter and height using gatoreye high-density UAS-LiDAR in an integrated crop-livestock-forest system. Remote Sens. 12.

Ferreira, M.P., de Almeida, D.R.A., de Almeida Papa, D., Minervino, J.B.S., Veras, H.F.P., Formighieri, A., Santos, C.A.N., Ferreira, M.A.D., Figueiredo, E.O., Ferreira, E.J.L., 2020. Individual tree detection and species classification of Amazon palms using UAS images and deep learning. For. Ecol. Manag. 475, 118397 https://doi.org/10.1016/j.foreco.2020.118397.

Ferreira, M.P., Lotte, R.G., D'Elia, F.V., Stamatopoulos, C., Kim, D.H., Ribeiro, M.B.N., Benjamin, A.R., 2021. Accurate mapping of Brazil nut trees (*Bertholletia excelsa)* in Amazon forests using worldview-3 satellite images and convolutional neural networks (vol 63, 101302, 2021). Ecol. Inform. 64.

Grybas, H., Congalton, R.G., 2021. A comparison of multi-temporal RGB and multispectral UAS imagery for tree species classification in heterogeneous New Hampshire forests. Remote Sens. 13, 2631.

He, K., Zhang, X., Ren, S., Sun, J., 2016. Deep residual learning for image recognition. In: The IEEE Conference on Computer Vision and Pattern Recognition (CVPR), pp. 770–778. https://doi.org/10.1109/CVPR.2016.90.

He, K., Gkioxari, G., Doll´ar, P., Girshick, R., 2017. Mask r-cnn. In: Proceedings of the IEEE International Conference on Computer Vision, pp. 2961–2969.

Hurtik, P., Molek, V., Hula, J., Vajgl, M., Vlasanek, P., Nejezchleba, T., 2022. Poly-yolo: higher speed, more precise detection and instance segmentation for yolov3. Neural Comput. & Applic. 34, 8275–8290.

Kattenborn, T., Leitloff, J., Schiefer, F., Hinz, S., 2021. Review on convolutional neural networks (CNN) in vegetation remote sensing. ISPRS J. Photogramm. Remote Sens. 173, 24–49. https://doi.org/10.1016/j.isprsjprs.2020.12.010.

Liu, H., 2022. Classification of urban tree species using multi-features derived from four-season RedEdge-MX data. Comput. Electron. Agric. 194, 106794.

Martins, G.B., La Rosa, L.E.C., Happ, P.N., Coelho Filho, L.C.T., Santos, C.J.F., Feitosa, R. Q., Ferreira, M.P., 2021. Deep learning-based tree species mapping in a highly Modzelewska, A., Kami´nska, A., Fassnacht, F.E., Stere´nczak, K., 2021. Multitemporal hyperspectral tree species classification in the białowie˙ za forest world heritage site. Forestry 94, 464–476.

Morales, G., Kemper, G., Sevillano, G., Arteaga, D., Ortega, I., Telles, J., 2018. Automatic segmentation of *Mauritia flexuosa* in unmanned aerial vehicle (UAS) imagery using deep learning. Forests 9. https://doi.org/10.3390/f9120736.

Murphy, K.P., 2012. Machine Learning: A Probabilistic Perspective. MIT press. Natesan, S., Armenakis, C., Vepakomma, U., 2020. Individual tree species identification using dense convolutional network (DenseNet) on multitemporal rgb images from uas. J. Unmanned Vehicle Syst. 8, 310–333.

Nuijten, R., Coops, N., Goodbody, T., Pelletier, G., 2019. Examining the multi-seasonal consistency of individual tree segmentation on deciduous stands using digital aerial photogrammetry (DAP) and unmanned aerial systems (UAS). Remote Sens. 11, 739. URL: https://doi.org/10.3390/rs11070739.

Onishi, M., Ise, T., 2021. Explainable identification and mapping of trees using UAS RGB image and deep learning. Sci. Rep. 11. URL: https://doi.org/10.1038/s41598-02 0-79653-9.

Ramos, A.M., Dos Santos, L.A.R., Fortes, L.T.G., 2009. Normais climatológicas do brasil, 1961-1990. Instituto Nacional de Meteorologia-INMET.

Tochon, G., F´eret, J., Valero, S., Martin, R., Knapp, D., Salembier, P., Chanussot, J., Asner, G., 2015. On the use of binary partition trees for the tree crown segmentation of tropical rainforest hyperspectral images. Remote Sens. Environ. 159, 318–331. https://doi.org/10.1016/j.rse.2014.12.020.

Veloso, H.P., Rangel-Filho, A.L.R., Lima, J.C.A., 1991. Classificaçãoo da vegetação 600 brasileira, adaptada a um sistema universal. Instituto Brasileiro de Geografia e Estatística.

Wagner, F.H., Ferreira, M.P., Sanchez, A., Hirye, M.C., Zortea, M., Gloor, E., Phillips, O. L., de Souza Filho, C.R., Shimabukuro, Y.E., Aragão, L.E., 2018. Individual tree crown delineation in a highly diverse tropical forest using very high resolution satellite images. ISPRS J. Photogramm. Remote Sens. 145, 362–377. https://doi.org/10.1016/j.isprsjprs.2018.09.013. sI: Latin America Issue.

Zhang, L., Zhang, L., Du, B., 2016. Deep learning for remote sensing data: a technical tutorial on the state of the art. IEEE Geosci. Remote Sens. Mag. 4, 22–40. https://doi.org/10.1109/MGRS.2016.2540798.

Appendix

Code construct and train the DeepLabV3+ model to classify commercial tree species

```
% To train the model you will need two images 'imgLabel' is the reference labeled image and 'img' is the RGB image. Include the path location of these images on the variables 'locationTrain' and 'locationTrainLabel' below. The functions randomPatchExtraction Datastore will automatically extract patches from the RGB and labeled image to train the model. Prediction is performed using the function 'segmentImagePatchWiseClassification BlockProcessing'. Please note that the model is trained with a predefined set of classes. If you want to ignore a given class during training, please use the 'standardizeMissing' function. For example, you can set the background class to '99' and ignore this class in the backpropagation altogrithm using imgLabel = standardize Missing(imgLabel,99). All pixels equal 99 in the labeled image will be ignored in the training process.

[imgLabel, ~] = readgeoraster('...'); labelIDs=unique(imgLabel(:));

        % State the folders names in which the RGB image and the training images are stored

locationTrain = '';
locationTrainLabel = '';

        % Create an ImageDatasote object

imds = imageDatastore(locationTrain,'FileExtensions',{'.tif'});

        % Get the number of classes in the training set labelIDs=1:17; % number of species

labelIDs = labelIDs(2:end,:);
classes =[];
        for i=1:size(labelIDs,1)
fileNameTest=['Tree_',num2str(i)];
classes{i,1}=fileNameTest;
        end

        % Create a pixelLabelDatastore object

pxds = pixelLabelDatastore(locationTrainLabel,classes,labelIDs);

        % Count the number of pixels in each class to compute the class weights

tbl = countEachLabel(pxds);

        % Specify the network image size.
```

```
pathSize = 256;
imageSize = [pathSize pathSize 3];

    % Specify the number of classes.

numClasses = numel(classes);

    %Create DeepLab v3+ for semantic segmentation

lgraph = deeplabv3plusLayers(imageSize, numClasses, "resnet18",'DownsamplingFactor',16);

    % Train model with more bands https://www.mathworks.com/
matlabcentral/answers/562448-resnet50-on-multi-spectral-image-segmentation


layers = lgraph.Layers;
lgraph = replaceLayer(lgraph,'data',imageInputLayer([pathSize pathSize
Nbands],'Name','input'));
lgraph = replaceLayer(lgraph,'conv1',convolution2dLayer(7,64,'stride',[2 2],'padding',[3 3 3
3],'Name','conv1'));


    % Balance Classes Using Class Weighting

imageFreq = tbl.PixelCount ./
tbl.ImagePixelCount; classWeights =
median(imageFreq) ./ imageFreq;

    % Specify the class weights using a pixelClassificationLayer.

pxLayer = pixelClassificationLayer('Name','labels','Classes',tbl.Name,'ClassWeights',
classWeights);

lgraph = replaceLayer(lgraph,"classification",pxLayer);

    % The layer automatically ignores undefined pixel labels during training.

analyzeNetwork(lgraph)

    % Check if everythin is ok!

    clc
```

```
        % Define training options.
        % Select a learning rate that is proportional to the mini-batch size and reduce the
learning rate by a factor of 10 after 60 epochs.

miniBatchSize = 12;

        % learnRate = 0.1*miniBatchSize/128;


learnRate=0.01;

        % Data augmentation during training

augmenter = imageDataAugmenter(  ...
                'RandRotation',[-20,20],  ...
                'RandXTranslation',[-5  5],  ...
                'RandYTranslation',[-10  10]);

        % Random patch extraction datastore

PatchSize=[pathSize pathSize];
dsTrain = randomPatchExtractionDatastore(imds,pxds,PatchSize,'PatchesPerImage',
500,'DataAugmentation',augmenter);

        % inputBatch = preview(dsTrain);
        % disp(inputBatch)
        % dsVal = randomPatchExtractionDatastore(imds,pxds,PatchSize,'PatchesPerImage',
100);

 options = trainingOptions('sgdm', ... 'Momentum',0.9,... 'ExecutionEnvironment','gpu',...
       'LearnRateSchedule','piecewise',... 'InitialLearnRate',learnRate, ...
       'LearnRateDropFactor',0.5, ... 'LearnRateDropPeriod',5, ... 'MaxEpochs',15, ...
       'MiniBatchSize',miniBatchSize, ...'Shuffle','every-epoch', ... 'GradientThreshold',0.05,...
       'VerboseFrequency',2,... 'Plots','training-progress',... 'ValidationPatience', 4);
         [net,~] = trainNetwork(dsTrain,lgraph,options);

        %% Perform semantic segmentaion with trained model

[img, R] = readgeoraster('...');
x=geotiffinfo('...');
S=struct([x.GeoTIFFTags.GeoKeyDirectoryTag]);
patchSize=[1024  1024];

        % Use block processing because the image is too big


block_size=[15000 15000];
```

```
SemanticSegFun = @(block_struct)segmentImagePatchWiseClassificationBlock Processing
(block_struct.data,net, patchSize);

        % Create a function handle

        out = blockproc(img,block_size,SemanticSegFun,'UseParallel',true,
'DisplayWaitbar',false);%%
function [out] = segmentImagePatchWiseClassificationBlock Processing(im,net, patchSize)

        %  This function performs patchwise semantic segmentation on the input image using
the provided network. The segmentation is performed patches-wise on patches of size
PATCHSIZE. NOTE: The function  also outputs a probability map showing the class
membership  probabilities for each class nclass is the number of classes

[height, width, nChannel] = size(im);
patch = zeros([patchSize, nChannel], 'like', im);

        % pad image to have dimensions as multiples of patchSize

padSize(1) = patchSize(1) - mod(height, patchSize(1)); padSize(2) =
patchSize(2) - mod(width, patchSize(2));
im_pad = padarray (im, padSize, 0, 'post'); [height_pad, width_pad, ~] = size(im_pad);
out = zeros([size(im_pad,1), size(im_pad,2)], 'double');

        % outProb = zeros([size(im_pad,1), size(im_pad,2)], 'double');
        % iter=0

 for i = 1:patchSize(1):height_pad for

       j =1:patchSize(2):width_pad

                    for p = 1:nChannel

                          patch(:,:,p) = squeeze(im_pad( i:i+patchSize(1)-1,...
                    end

        %       iter=iter+1

[patch_seg,~,~] = semanticseg(patch, net, 'outputtype', 'double'); out(i:i+patchSize(1)-1,

j:j+patchSize(2)-1) = patch_seg;

       % outProb(i:i+patchSize(1)-1, j:j+patchSize(2)-1) = scores;
        % outProbClass(i:i+patchSize(1)-1, j:j+patchSize(2)-1,:) = allScores; end
          end
```

```
% Remove the padding

out = uint8(out(1:height, 1:width));

% outProb=outProb(1:height, 1:width);
% outProbClass=outProbClass(1:height, 1:width,:);

end
```

CHAPTER 2

ESTIMATING COMMERCIAL TREE VOLUME BASED ON CROWN MAPPING BY UAS IMAGENS IN THE AMAZON FOREST*

*Chapter formatted to Scientific Electronic Archives.

ESTIMATING COMMERCIAL TREE VOLUME BASED ON CROWN MAPPING BY UAS IMAGENS IN THE AMAZON FOREST

Hudson Franklin Pessoa Veras[a]∗, Ernandes Macedo da Cunha Neto[a], Iací Dandara Santos Brasil[a], João Paulo Sardo Madi[a], Emmanoella Costa Guaraná Araujo[b], Jorge Danilo Zea Camaño[c], Evandro Orfanó Figueiredo[d], Daniel de Almeida Papa[d], Matheus Pinheiro Ferreira[e], Ana Paula Dalla Corte[a], Carlos Roberto Sanquetta[a]

[a]Departament of Forest Science, Federal University of Paraná (UFPR), Pref. Lothário Meissner Avenue 900, 80210-170 Curitiba-PR, Brazil
[b]Departament of Forest Science, Federal University of Rondônia (UNIR), Av. Pres. Dutra, 2965 - Olaria, 76801-058, Rolim de Moura-RO, Brazil
[c]Grupo SECC (Servicios Ecosistémicos y Cambio Climático), Ministerio de Ciencia Tecnología e Innovación de Colombia [d]Embrapa Acre, Rodovia BR-364, km 14, 69900-056 Rio Branco-AC, Brazil
[e]Cartographic Engineering Department, Military Institute of Engineering (IME), Praça Gen. Tibúrcio 80, 22290-270 Rio de Janeiro-RJ, Brazil

∗Corresponding author
Email address: hudsonveras@gmail.com (Hudson Franklin Pessoa Veras)

ABSTRACT

The use of remote sensing images obtained by unmanned aerial vehicle (UAS) systems enables measuring the morphometry of the tree canopy to estimate the volume stock in the Amazon forest. Application of RGB images from UAS systems to capture the dendrometry of trees in native forest is still poorly understood. In this study, we used RGB images from a low cost UAS to map tree species and extract volumetric stock estimates in an Amazon forest. Individual tree crowns (ITC) were outlined in the UAS images and identified to the species level using forest inventory data. The average diameter and crown area of the trees were measured to estimate the volume, basal area and DBH per diameter class for 260 ha of tropical forest. The RMSE volume adjustment for the separate field inventory dataset was 19.31% with an R2 of 0.967. The UAS system images has the potential to map tree species and estimate tree dendrometry attributes in the Amazon Forest, providing valuable insights for forest management and conservation.

Keywords: RGB images, diameter class, orthomosaic, tropical forest.

1. Introduction

The forest volume is essential to determine the biomass, which constitutes an element responsible for reducing the emission of greenhouse gases and has the capacity to fix atmospheric carbon during its formation process. Tropical forests have high diversity and dynamic characteristics, with constant changes in their structure that require complex planning to execute forestry operations (Coops et al., 2022).

The traditional forest inventory is indispensable for monitoring forests, as it seeks to monitor and portray changes in the quantitative and qualitative attributes of the arboreal environment (Latifi and Heurich, 2019; Fankhauser et al., 2018a; Tompalski et al., 2021) In turn, these attributes are necessary to support accurate diversity, volume and estimates biomass, being an important tool to assess important aspects such as productivity and the economic and ecological viability of interventions to be conducted in a region, thereby encouraging decision-making by environmental managers (Keenan et al., 2015).

The use of geotechnologies applied in forests for identifying species, biomass and carbon, conservation, monitoring, impact assessment and even tree dendrometric attributes is being used more and more frequently (Corte et al., 2022; Moura et al., 2021; da Cunha Neto et al., 2021; da Costa et al., 2021; d'Oliveira et al., 2020; Fankhauser et al., 2018b). Os Unmanned Aircraft Vehicle (UAS) with RGB sensors images in the red, green and blue bands, are low cost equipment with great demand and supply in the market due to their various uses, and are becoming popular in the forestry sector for use as support in data collection operations, inspection activities and coverage monitoring, among others.

UAS-based data acquisition usually results in hundreds of high spatial resolution RGB images with ground sampling distance (GSD) under 10 cm (Ferreira et al., 2020; Kattenborn et al., 2021; Morales et al., 2018). The combination of remote sensing and forest inventory data provides accurate information about forest characteristics over large areas (hundreds hectares) and has been shown to be useful in reducing field efforts (de Almeida Papa et al., 2020; Dalla Corte et al., 2020; Veras et al., 2022).

In traditional forest measurement by census or sampling, the measurement of diameter at breast height (DBH) and total height (h) of trees are generally used due to the high correlation of these variables with parameters such as wood volume and carbon stock (Corte et al., 2020). Data collection is time-consuming, has high costs, low productivity, is restricted to small areas and dangerous to the health of the field worker, and may still encounter geographic obstacles and still risk data collection errors (Latifi, 2020).

The measurement and identification of trees using a UAS system significantly reduces the need for a traditional forest inventory, which contributes to optimizing financial resources, time, labor, planning and forest management, enabling identification of tree distribution, tree density, species, individual counts, monitoring forest phenophases, in addition to tree biometrics (Veras et al., 2022).

In view of the above, this study examines the utility of RGB images captured by a UAS system to map and to estimate the volume of tree species in Brazilian Amazon forests. Specifically, we tested the hypothesis that is possible estimate the tree volume commercial from aerial mapping using a UAV system with RGB sensor. And, additionally, estimate diameter and basal area from the canopy morphometry of large arboreal trees present in the Amazon forest.

2. Materials

2.1. Study area

The study area is an experimental forest of the Brazilian Agricultural Research Company (Embrapa) located in the municipality of Rio Branco, Acre state, Brazil (10º 01’ 22" S, 67º 40’ 3" W) (Fig 1). It is a highly diverse native rain forest area of 1,600 ha about 200 m above the sea level, more than 239 species already cataloged. The orthomosaic used in this study comprises 260 ha. The experimental forest area annually receives 1,950 mm of rain, and the annual average temperature is 24.8 (±0.8)ºC (Ramos et al., 2009). The vegetation of the area is classified as open rain forest with the presence of palms and bamboos (ACRE, 2010). Trees exceed 30 meters in height, and there is an abundance of bamboo and diversity of palm trees, along with tree individuals in lower density, and the presence of large trees.

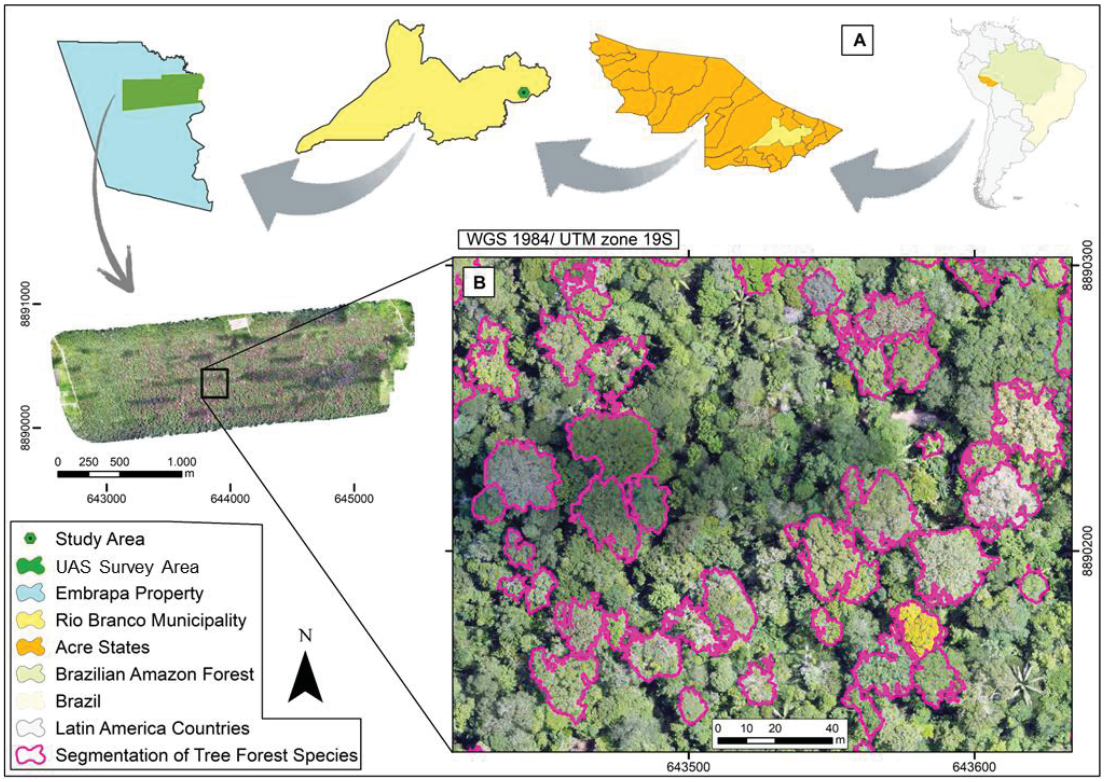

Fig. 1. (A) Location of the study area in the Acre state, southwestern Amazon, Brazil. (B) Segmentation of tree forest species in the native forest

2.2 UAS photographs

We collected aerial photographs with the UAS DJI Phantom 4 Pro, equipped with an RGB (red, green, blue) CMOS sensor of 20-megapixel resolution, a 24 mm autofocus lens, and a manual shutter with battery autonomy up to 30 min. The UAS flew 120 m above the forest canopy with a cruising speed of 10 m/s, resulting in images with a GSD (Ground Sample Distance) of 4 cm. We took a total of 1,585 photographs with a forward overlap of 86.0% and side lap of 86.36% in eight consecutive flights. All images were captured in manual shutter mode, speed 1/500 and diaphragm setting 6.0, which is the necessary setting to avoid rolling shutter in images. Before the flights, we established three ground control points (GCPs) on the edges of the forest reserve. Ten sequential flights were performed to map the entire study area in different months. A dual-frequency GNSS receiver was installed at each GCP and collected GPS and GLONASS data for 241 minutes. After post-processing procedures, the average horizontal and vertical precision of the GCPs were 10 cm and 3 cm, respectively. We used GCPs to facilitate tree identification by crossing field inventory data, minimizing XY

displacement errors. Finally, we used the PiX4D® software program (Pix4D Inc.) to generate orthomosaics of the study area.

3 Methods

3.1 Individual tree crown (ITC) dataset

First, we measured and identified all trees with a diameter at breast height (DBH) greater than 50 cm to the species level in the forest inventory experimental area, the volume (m^3) of the trees was derived from the rigorous measurement of 1,500 trunks in a wood storage yard, with input of the DBH and H (commercial) variables into an equation generated by the Embrapa Acre research institution (Almeida Papa, 2020).

Volume Equation:

$$V = -0{,}225042 + 0{,}697672(DBH^2) + 0{,}638055((DBH^2)H) + 1{,}41241(H^{0,5})$$

R^2: 90.3223

$Syx_{(\%)}$: 20.58

For this study, we selected the most economically important species for nut and timber production and delineated their ITCs in the UAS images.

We performed the segmentation of each ITC using the Definiens Ecognition® software program, in which a greater weight was applied to the image pixel and a smaller one to the texture; each orthomosaic has different characteristics, so it was necessary to adjust the weight for each image. Then we filtered with the trees from the field forest inventory and excluded the non-whole crowns. ITC delineation was carefully performed so that a single ITC polygon encompasses the same tree. We outlined a total of 388 ITCs, corresponding to 55 species. According to the forest inventory, the DBH of the inventoried trees ranged from 50.0 cm to 190.0 cm, with the total height of some trees reaching 40 m. A greater number of individuals and height estimation resulting from the difference between the Digital Surface Model of the UAS and Digital Terrain Model can be seen in the smallest diametric classes (Table 1),

constituting similar behavior to a mature forest without anthropic intervention (Meyer, 1952; Assmann, 1970).

Table 1: Diametric distribution and estimated average height of trees from UAS considered to estimate volume through crown morphometry using UAS.

Diametric class	N. Tree	UAS (m)	%
50|- 60	61	28,02	15,76
60|- 70	57	29,89	14,73
70 |- 80	49	30,33	12,66
80 |- 90	47	30,86	12,14
90 |- 100	43	32,87	11,11
110 |- 120	37	33,97	9,56
120 |- 130	28	35,05	7,24
130 |- 140	20	35,84	5,17
140 |- 150	16	35,67	4,13
150 |- 160	12	35,48	3,10
160 |- 170	10	36,45	2,58
> 170	7	36,82	1,81

3.1.1 UAS-derived variables

We derived canopy morphometry metrics, variable area (ca) and diameter (cd) from the UAS images; the crown diameter was obtained from the average between the largest and smallest diameter of each sample (Fig 2) adapted from Figueiredo et al. (2014).

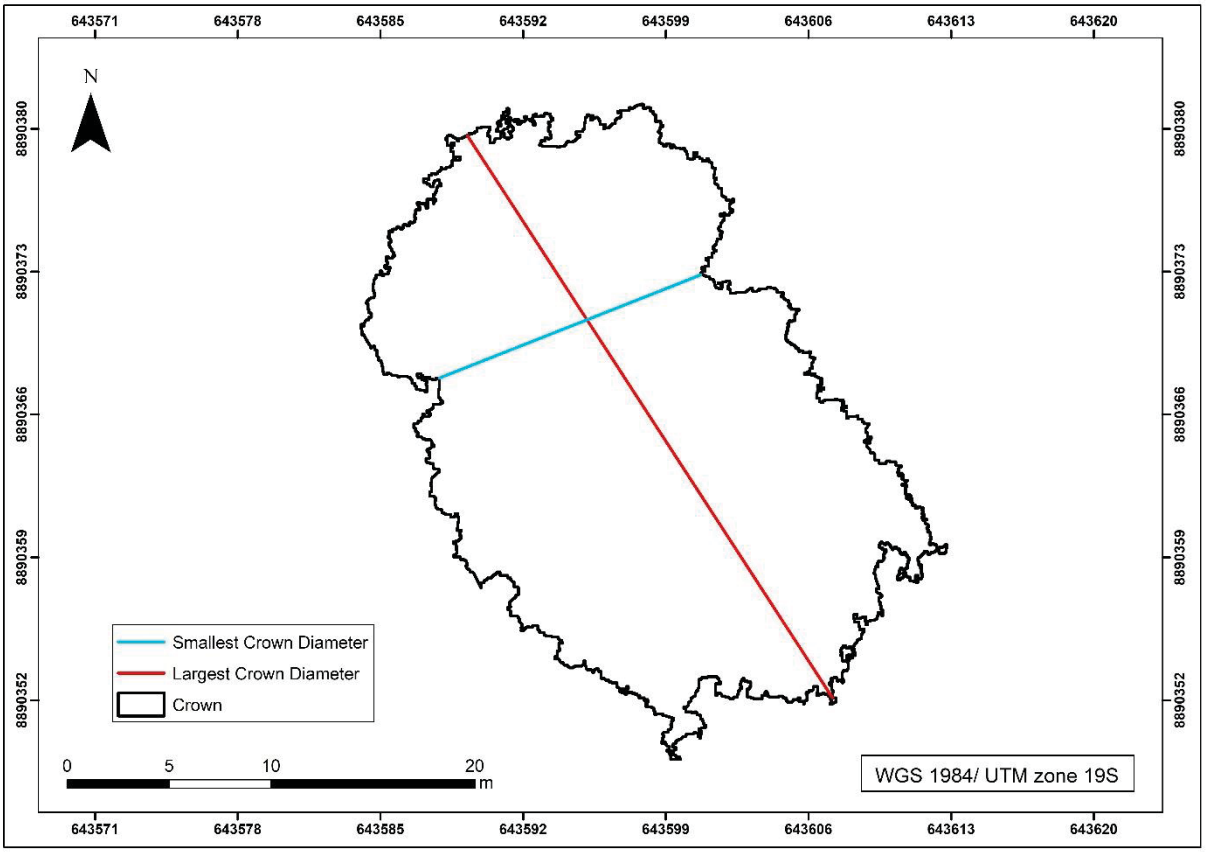

Fig. 2. Example of a sample of the average tree crown diameter (cd) obtained by averaging the largest and smallest diameter

3.2 Predicted dendrometric parameters based on UAS-derived variables

We subdivided the dataset into 70% for fitting and 30% to validate the models, which is a division based on research in similar works. We selected the independent regression variables based on their correlation with the dependent variables (volume - V, basal area - G, and DBH). The morphometric diameter and crown area variables obtained a strong correlation with volume, basal area and DBH, which were selected to compose the regression model. The statistical analysis was conducted in R language programming with used package metrics and corplot (R Core Team, 2021).

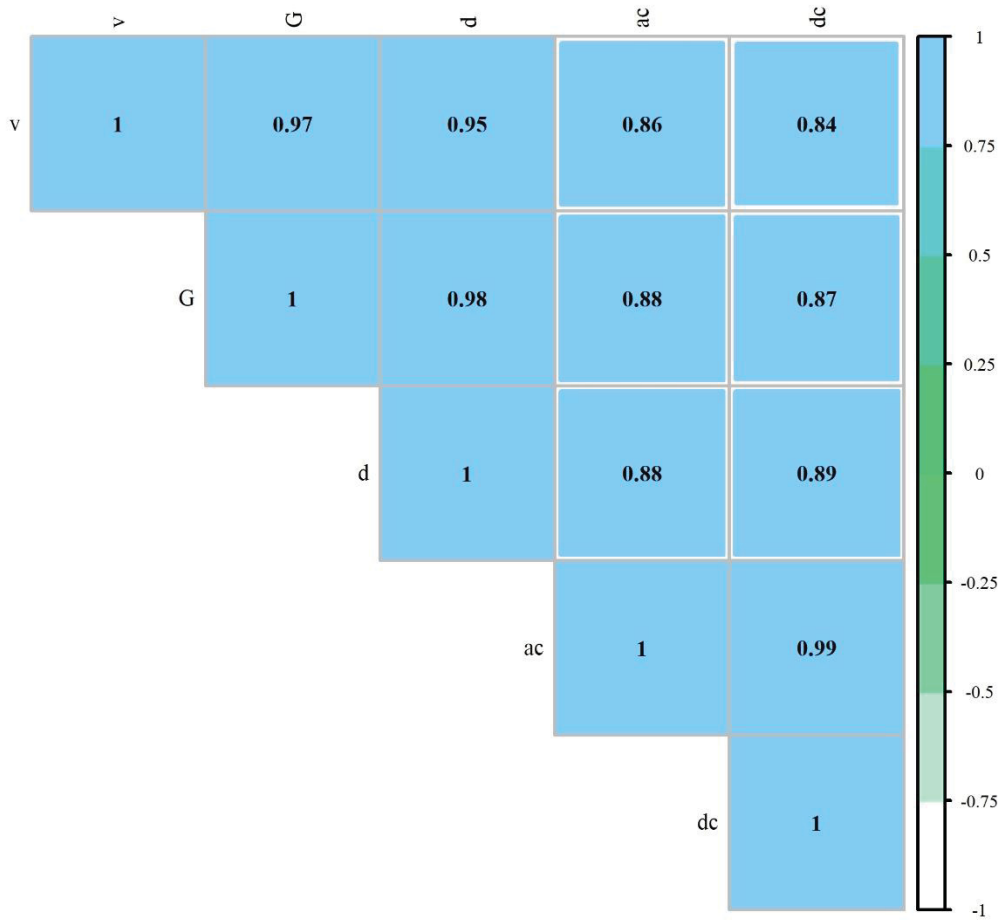

Fig. 3. Correlation chart between dendrometric and UAS derived variables

*Note: v is the tree volume, G is the tree basal area, DBH is the tree diameter at breast height, ca is crown area, cd is crown diameter.

Next, we fitted three linear regression models using volume, basal area, and DBH as dependent variables and the diameter and canopy area as independent variables (Models 1 - 3). We decided to use the tree's diametric class as a categorical variable in order to increase the model accuracy.

$$V = \beta_0 + \beta_1 ca + \beta_2 cd + \beta_i DC_i \quad (1)$$

$$G = \beta_0 + \beta_1 ca + \beta_i DC_i \quad (2)$$

$$DBH = \beta_0 + \beta_1 cd + \beta_i DC_i \quad (3)$$

In which: βi are the model parameters, ca is the crown area, cd is the crown diameter, DC is the diameter class.

3.3. Accuracy assessment

The models' fit was evaluated by the adjusted determination coefficient (R^2), standard estimate error (SEE), and the residual plot, while the model generalization at the validation database was evaluated by the Pearson's correlation coefficient, the root mean square error, paired T-test, and the residual plot.

4 Results

The volume (v) predictions had metrics on the fit and validation respectively, with SEE of 21.97% for the fit and RMSE 19.13%. In addition to an R^2 greater than 0.90 in both cases. On the other hand, the basal area (G) and diameter (DBH) estimates had high statistical metrics, with a SEE < 6.5% and $R^2 > 0.99$, denoting the model's accuracy, as well as the potential and the canopy variables' potential for determining these variables (Table 2).

Table 2: Models' statistical metrics

Variable	Statistical analysis						
	FIT			Test			
	R^2	SEE	SEE (%)	r	RMSE	RMSE (%)	T (p-value)
V	0.916	2.507	21.972	0.967	2.124	19.314	0.04ns
G	0.992	0.045	6.231	0.995	0.052	7.297	0.07ns
DBH	0.993	2.559	2.820	0.995	2.876	3.183	0.02ns

In which: V is volume, G is basal area, DBH is diameter at breast height, R^2 is adjusted determination coefficient, SEE is standard estimate error, r is Pearson's linear correlation, RMSE is root mean square error, T is the Paired T-test, ns is non-significance.

Only the volume residuals are heteroscedastic, while G and DBH residuals are between -25% and 25%, which demonstrates accuracy (Figure 4). The residual's fit (Figure 4b) obtained a greater variation than the validation. These performances reflected the model's statistical metrics.

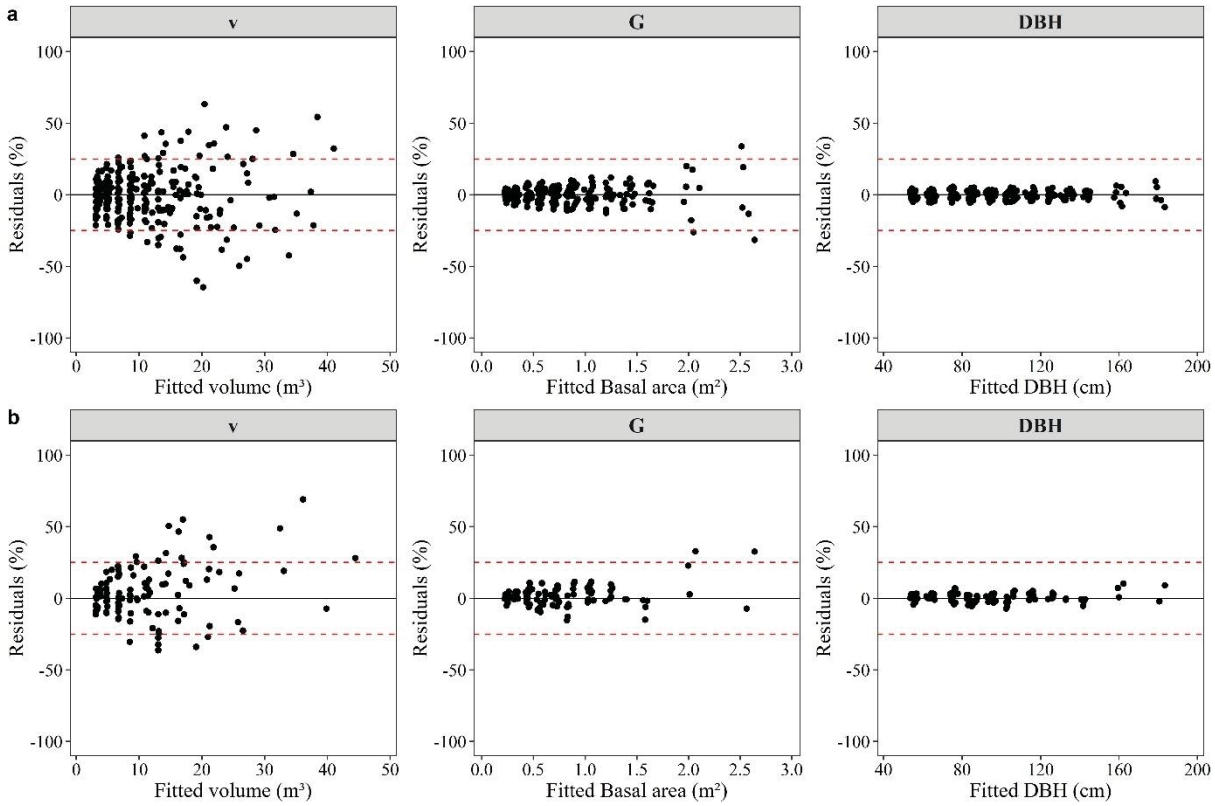

Fig. 4. Fit and validation residual plot

Note: a is the fit residuals plot, and b is the validation residuals plot.

The models' accuracy is observed in the correlation plot, in which the volume had a greater variation of observed vs. estimated values, although the regression model's mean line of fit (red line) passes close to the perfect correlation (dashed black line). G and DBH obtained lower variation, with points next to the regression model and the perfect correlation (Figure 5).

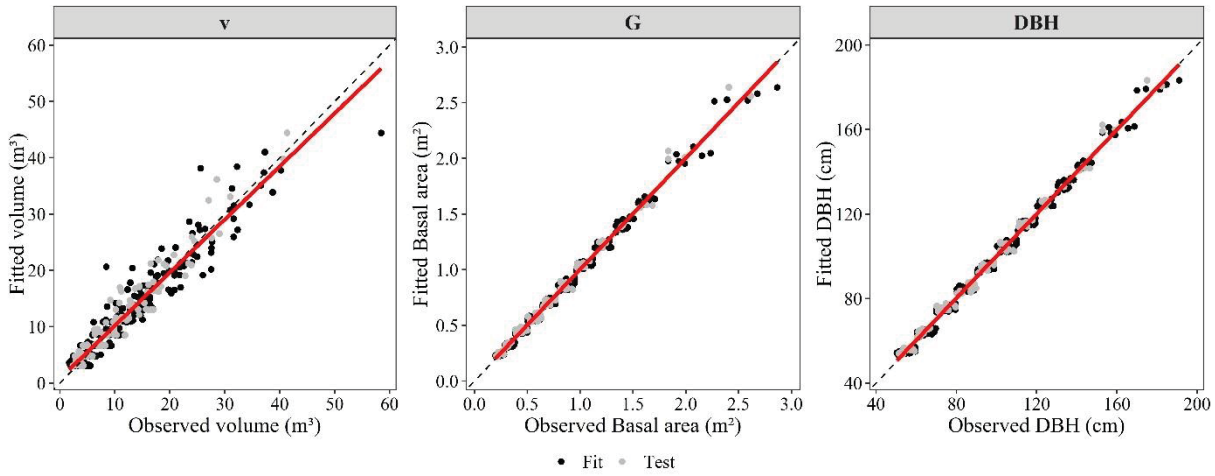

Fig. 5. Dendrometric variables' accuracy on fit and validation dataset

Dendrometric variables' accuracy for the fit and validation dataset. The models' coefficients are significant in all the estimated variables, explaining the intercept (β_0) variation and the inclinations on the regression curves throughout the diameter classes, indicating there are different inclinations among the diameter classes which explain the tree volume behavior based on the crown variables (Table 3).

Table 3: Coefficients of the variables used to adjust the models

Parameter	V	G	DBH
β_0	12.254*	0.186*	46.390*
β_1	0.043*	0.00035*	0.633*
β_2	-1.117*	0.073*	8.215*
β_3	1.676*	0.181*	18.297*
β_4	3.560*	0.291*	27.233*
β_5	5.430*	0.418*	36.332*
β_6	7.717*	0.561*	45.601*
β_7	9.949*	0.729*	55.283*
β_8	12.748*	0.867*	62.897*
β_9	14.589*	1.057*	72.171*
β_{10}	16.519*	1.251*	80.970*
β_{11}	21.376*	1.619*	96.342*
β_{12}	26.030*	2.133*	115.421*
β_{13}	30.830*	-	-

Note: V is volume, G is basal area, DBH is diameter at breast height, βi is the model parameter, * is significance. Regarding the volume estimates, β1 was associated with crown area and β2

with crown diameter, β3 to β13 were associated the 11 diameter class coefficients. For the G and DBH estimate β2 to β12 were associated the 11 diameter class coefficients. For the G estimates, β1 was associated with crown area, and with crown diameter for DBH. The diameter class 1 was associated to β0 for all variables

5. Discussion

The tree crown segmentation using the UAS with RGB sensors proved to be feasible, as it is a low cost equipment which enables extracting the variables crown area (ac) and crown diameter (cd) and relate them to variables which are difficult to measure: DBH, basal area and volume.

In this study, the variables v, G, DBH, ca and cd were strongly correlated with each other (Figure 3), evidencing their importance in the estimates by equations (1-3). The strong correlation is in agreement with the study by Iizuka et al. (2018), in which it is mentioned that the variables DBH, area and crown diameter are highly correlated with the individual diameters of the trees.

Obtaining the tree volume is a limiting factor for operational planning in forest management and forest biomass, in which the use of morphometric variables of the crown tend to improve the accuracy of estimates from the UAS (Figueiredo et al., 2014), which confirms the high degree of correlation between canopy variables and volume. DBH is another variable to be considered when estimating volume (Tudoran et al., 2021) due to its high correlation, which is evidenced in this study.

The fitting of the volume model that relates the crown variables and the diametric class proves to be an efficient way for its estimation. The results related to the volume model fit statistics (Table 2) were lower than the studies by Tudoran (2022) (RMSE ≈ 9%) and by Figueiredo et al. (2014) (RMSE = 16.73%). The superiority of the cited studies in addition to the different models used can be explained by being associated with characteristics related to the forest rather than the individual characteristics of the trees, such as DBH, height and crown size, which vary167 in relation to the tree stand structure. The inferiority of the calculated statistics, mainly in relation to the study by Tudoran et al. (2021), can be explained by the specificity of the study area, since the Amazon forest has a high degree of complexity which entails a greater variability of the Biometric characteristics of trees.

Therefore, the influence of structure and local conditions in trees should be taken into account when developing models based on biometric variables (Tudoran et al., 2021; Guerra-

Hernández et al., 2016). In turn, models that express the relationship between the dendrometric characteristics of trees need to be developed separately for each type of structure.

Figueiredo et al. (2014) found that models using variables exclusively from the canopy revealed $R^2_{aj.}$(%), results ranging from 72,68 to 79,44 and percentage standard error between 27,47% to 30,84%, which were lower than those models that included the DBH as one of the independent variables, and constituting similar results to the simple entry equations in dendrometric studies in the Amazon. According to the same author, none of the generated models that exclusively use the traditionally employed independent variables (DBH, Ht) obtained better results than models that also apply variables derived from the crown morphometry indices.

The study revealed satisfactory results for the 3 models. The fits of the diameter and basal area models present superior statistics according to the R^2 and SEE values. This can be explained since the DBH and G are variables with a lower degree of uncertainty when measured directly than the volume that is a variable estimated. The fits were satisfactory according to the analyzed statistics when comparing the results obtained with other studies. Tudoran (2022) found an RMSE of 13.7%, which can be explained by the use of the cd variable only as a linear function in estimating the diameter, and the diameter classes in the model in this study were associated in addition to cd. When Tudoran et al. (2021) used a third-degree polynomial function using cd as a variable, it resulted in RMSE values which varied between (0.32 – 0.89). This difference in the goodness of fit can be explained by the difference in forest density that influences the DBH-cd relationship.

Despite the results found showing great efficiency in estimating variables resulting from crown morphometry, one of the major limitations in indirect estimations through data capture with passive sensors coupled to UASs is penetration into dense forests, resulting in partial detection or omission of smaller trees shaded by larger trees, limiting the data collection from the understory (for example), as pointed out by Iizuka et al. (2018) in their tree segmentation study.

Collecting good aerial images with an RGB sensor to accurately define the treetops is still a difficult task. It is necessary to take some precautions: mapping with the UAS in the hours of greatest luminosity, adjusting the camera shutter for fast shooting (>1/500) and the high diaphragm to be more accurate in correctly focusing the target (>6.0). The aerial images will be very clear without the rolling shutter effect from following these settings, able to extract more accurate information, even with the existing limitations of the segmentation of the cd and ca variables from the UAS. The inference of hard-to-obtain dendrometric variables such as

volume decreases operating costs in forest inventories, in addition to only needing information from larger trees for decision-making, for example in sustainable forest management.

Studies have achieved satisfactory results by segmenting trees from UAS data with spacing between objects (Veras et al., 2022; Tudoran et al., 2021; Torres et al., 2020; Huang et al., 2018; Lin et al., 2015; Torres-Sánchez et al., 2015). The segmentation of trees to obtain dendrometric variables from UAS data in a natural dense forest is complex due to the proximity between tree canopies; data from active sensors, such as LiDAR, generally have better performance to segment the tree canopy and characterize the tree stock (Torresan et al., 2020; Figueiredo et al., 2014; Yan et al., 2018).

The use of remote technologies is a strong ally for decision-making by the environmental manager. This study has the role of providing information quickly at a reduced cost and from large areas, while the use of canopy variables with a high degree of association with volume, basal area and DBH provided accurate estimates, which infers that we should seek alternatives of using these variables in order to make the forest inventory less onerous and maintain its accuracy. Thus, remote RGB sensors can help as complementary tools to the forest inventory, making it possible to reduce sampling units in the field and adapt models for the entire area based on morphometric variables of the tree canopy.

6. Conclusions

In this work, we have shown that the use of aerial images from a UAS system enables making indirect dendrometric estimates through tree canopy morphometry for the Amazon Forest. The equation for the variable volume composed by a combination of the area and crown diameter variables by diametric class had an admissible error in the context of inventories in natural tropical forests compatible with the field data of the forest inventory, with R^2 0.967 and RMSE 19.31%. The aerial mapping with UAS to extract information from the dendrometry attributes of the trees proved to be very useful to obtain a previous estimate of the tree stock of a forest, constituting important data for the environmental manager to plan the management and conservation of forest resources. Future studies will focus on applying this technique to other forest typologies to expand the study base and improve the accuracy of the models by using more accurate algorithms and image processing methods.

Acknowledgments

This study was funded in part by the Coordination for the Improvement of Higher Level Personnel (CAPES) - Finance Code 001 (A. Corte 88887.373249/2019-00), MC-371 TIC/CNPq No. 28/2018 (408785/2018-7; 438875/2018-4), CNPq No. 09/2018 (302891/2018-8).

References

de Almeida Papa, D., de Almeida, D.R.A., Silva, C.A., Figueiredo, E.O., Stark, S.C., Valbuena, R., Rodriguez, L.C.E., d' Oliveira, M.V.N., 2020. Evaluating tropical forest classification and field sampling stratification from LiDAR to reduce effort and enable landscape monitoring. Forest Ecology and Management 457, 117634. URL: https: //www.sciencedirect.com/science/article/pii/S037811271931179X, doi:https://doi.org/ 10.1016/j.foreco.2019.117634.

Acre. Governo do Estado do Acre. Zoneamento Ecológico-Econômico do Estado do Acre, Fase II (Escala 1:250.000): Documento Síntese. 2. Ed. Rio Branco: SEMA, 2010. 356p. 1. ACRE – Zoneamento Ecológico-Econômico, 2. Meio Ambiente – Socioeconomia – Cultural/Político, 3. Gestão Territorial – Acre, I. Título.

Assmann, E., 1970. The principles of forest yield: studies in the organic production, structure, increment and yield of forest stands. Pergamon Press.

Coops, N.C., Tompalski, P., Goodbody, T.R.H., Achim, A., Mulverhill, C., 2022. Framework for near real-time forest inventory using multi source remote sensing data. Forestry: An International Journal of Forest Research URL: https://doi.org/10.1093%2Fforestry% 2Fcpac015, doi:10.1093/forestry/cpac015.

Corte, A.P.D., da Cunha Neto, E.M., Rex, F.E., Souza, D., Behling, A., Mohan, M., Sanquetta, M.N.I., Silva, C.A., Klauberg, C., Sanquetta, C.R., Veras, H.F.P., de Almeida, D.R.A., Prata, G., Zambrano, A.M.A., Trautenmüller, J.W., de Moraes, A., Karasinski, M.A., Broadbent, E.N., 2022. High-density uas-LiDAR in an integrated crop-livestock forest system: Sampling forest inventory or forest inventory based on individual tree detection (itd). Drones 6. URL: https://www.mdpi.com/2504-446X/6/2/48, doi:10. 3390/drones6020048.

Corte, A.P.D., Souza, D.V., Rex, F.E., Sanquetta, C.R., Mohan, M., Silva, C.A., Zambrano, A.M.A., Prata, G., de Almeida, D.R.A., Trautenmüller, J.W., Klauberg, C., de Moraes, A., Sanquetta, M.N., Wilkinson, B., Broadbent, E.N., 2020. Forest inventory with high268 density UAS-LiDAR: Machine learning approaches for predicting individual tree attributes. Computers and Electronics in Agriculture 179, 105815. URL: https://doi.org/10.1016% 2Fj.compag.2020.105815, doi:10.1016/j.compag.2020.105815.

da Costa, M.B.T., Silva, C.A., Broadbent, E.N., Leite, R.V., Mohan, M., Liesenberg, V., Stoddart, J., do Amaral, C.H., de Almeida, D.R.A., da Silva, A.L., Goya, L.R.R.Y., Cordeiro, V.A., Rex, F., Hirsch, A., Marcatti, G.E., Cardil, A., de Mendonça, B.A.F., Hamamura, C., Corte, A.P.D., Matricardi, E.A.T., Hudak, A.T., Zambrano, A.M.A., Valbuena, R., de Faria, B.L., Junior, C.H.S., Aragao, L., Ferreira, M.E., Liang, J., de Pádua Chaves e Carvalho, S., Klauberg, C., 2021. Beyond trees: Mapping total aboveground biomass density in the brazilian savanna using high-density UAS-LiDAR data. Forest Ecology and Management 491, 119155. URL: https://doi.org/10.1016%2Fj.foreco.2021.119155, doi:10.1016/j.foreco.2021.119155.

da Cunha Neto, E.M., Rex, F.E., Veras, H.F.P., Moura, M.M., Sanquetta, C.R., Käfer, P.S., Sanquetta, M.N.I., Zambrano, A.M.A., Broadbent, E.N., Corte, A.P.D., 2021. Using high282 density uas-LiDAR for deriving tree height of araucaria angustifolia in an urban atlantic rain forest. Urban Forestry Urban Greening 63, 127–197. doi:10.1016/j.ufug.2021.127197.

Dalla Corte, A.P., Rex, F.E., Almeida, D.R.A.d., Sanquetta, C.R., Silva, C.A., Moura, M.M., Wilkinson, B., Zambrano, A.M.A., Cunha Neto, E.M.d., Veras, H.F.P., Moraes, A.d., Klauberg, C., Mohan, M., Cardil, A., Broadbent, E.N., 2020. Measuring individual tree diameter and height using gatoreye high-density UAS-LiDAR in an integrated crop-livestock-forest system. Remote Sensing 12. URL: https://www.mdpi.com/2072-4292/12/5/863, doi:10.3390/rs12050863.

d'Oliveira, M.V.N., Broadbent, E.N., Oliveira, L.C., Almeida, D.R.A., Papa, D.A., Ferreira, M.E., Zambrano, A.M.A., Silva, C.A., Avino, F.S., Prata, G.A., Mello, R.A., Figueiredo, E.O., Jorge, L.A.d.C., Junior, L., Albuquerque, R.W., Brancalion, P.H.S., Wilkinson, B., Oliveira-da Costa, M., 2020. Aboveground biomass estimation in Amazon tropical forests: a comparison of aircraft- and gatoreye uas-borne LiDAR data in the chico mendes extractive reserve in acre, brazil. Remote Sensing 12. URL: https://www.mdpi.com/ 2072-4292/12/11/1754, doi:10.3390/rs12111754.

Fankhauser, K., Strigul, N., Gatziolis, D., 2018a. Augmentation of traditional forest inventory and airborne laser scanning with unmanned aerial systems and photogrammetry for forest monitoring. Remote Sensing 10, 1562. URL: https://doi.org/10.3390%2Frs10101562, doi:10.3390/rs10101562.

Fankhauser, K., Strigul, N., Gatziolis, D., 2018b. Augmentation of traditional forest inventory and airborne laser scanning with unmanned aerial systems and photogrammetry for forest monitoring. Remote Sensing 10, 1562. URL: https://doi.org/10.3390%2Frs10101562, doi:10.3390/rs10101562.

Ferreira, M.P., de Almeida, D.R.A., de Almeida Papa, D., Minervino, J.B.S., Veras, H.F.P., Formighieri, A., Santos, C.A.N., Ferreira, M.A.D., Figueiredo, E.O., Ferreira, E.J.L., 2020. Individual tree detection and species classification of Amazon palms using UAS images

and deep learning. Forest Ecology and Management 475, 118397. doi:https://doi.org/10.1016/j.foreco.2020.118397.

Figueiredo, E.O., d'Oliveira, M.V.N., Fearnside, P.M., de Almeida Papa, D., 2014. Models to estimat e volume of individual trees by morphometry of crowns obtained with LiDAR. Cerne 20, 621–628. doi:10.1590/01047760201420041693.

Guerra-Hernández, J., Tomé, M., González-Ferreiro, E., 2016. Cartografía de variables dasométricas en bosques mediterráneos mediante análisis de los umbrales de altura e inventario a nivel de masa con datos LiDAR de baja resolución. Revista de Teledeteccion 2016, 103–117. doi:10.4995/raet.2016.3980.

Huang, H., Li, X., Chen, C., 2018. Individual tree crown detection and delineation from very-high-resolution UAS images based on bias field and marker-controlled watershed segmentation algorithms. IEEE Journal of Selected Topics in Applied Earth Observations and Remote Sensing 11, 2253–2262. doi:10.1109/JSTARS.2018.2830410.

Iizuka, K., Yonehara, T., Itoh, M., Kosugi, Y., 2018. Estimating tree height and diameter at breast height (dbh) from digital surface models and orthophotos obtained with an unmanned aerial system for a japanese cypress (*chamaecyparis obtusa*) forest. Remote Sensing 10. doi:10.3390/rs10010013.

Kattenborn, T., Leitloff, J., Schiefer, F., Hinz, S., 2021. Review on convolutional neural networks (CNN) in vegetation remote sensing. ISPRS J. Photogramm. Remote Sens. 173, 24–49. doi:https://doi.org/10.1016/j.isprsjprs.2020.12.010.

Keenan, R.J., Reams, G.A., Achard, F., de Freitas, J.V., Grainger, A., Lindquist, E., 2015. Dynamics of global forest area: Results from the FAO global forest resources assessment 2015. Forest Ecology and Management 352, 9–20. URL: https://doi.org/10.1016%2Fj.foreco.2015.06.014, doi:10.1016/j.foreco.2015.06.014.

Latifi, H., 2020. Remote sensing-assisted temperate forest inventories: a complement or an alternative? URL: http://rgdoi.net/10.13140/RG.2.2.30602.29121, doi:10.13140/RG.2.2.30602.29121.

Latifi, H., Heurich, M., 2019. Multi-scale remote sensing-assisted forest inventory: A glimpse of the state-of-the-art and future prospects. Remote Sensing 11, 1260. URL: https://doi.org/10.3390%2Frs11111260, doi:10.3390/rs11111260.

Lin, Y., Jiang, M., Yao, Y., Zhang, L., Lin, J., 2015. Use of UAS oblique imaging for the detection of individual trees in residential environments. Urban Forestry Urban Greening 14, 404–412. URL: https://www.sciencedirect.com/science/article/pii/S1618866715000333, doi:https://doi.org/10.1016/j.ufug.2015.03.003.

Meyer, H.A., 1952. Structure, growth, and drain in balanced uneven-aged forests. Journal of Forestry 2, 85–92.

Morales, G., Kemper, G., Sevillano, G., Arteaga, D., Ortega, I., Telles, J., 2018. Automatic segmentation of Mauritia flexuosa in unmanned aerial vehicle (UAS) imagery using deep learning. Forests 9. doi:10.3390/f9120736.

Moura, M.M., Oliveira, L.E.S., Sanquetta, C.R., Bastos, A., Mohan, M., Dalla Corte, A.P., 2021. Towards amazon forest restoration: Automatic detection of species from UAS imagery. Remote Sensing 13. URL: https://www.mdpi.com/2072-4292/13/13/2627, doi:10.3390/ rs13132627.

R Core Team, 2021. R: A Language and Environment for Statistical Computing. R Foundation for Statistical Computing. Vienna, Austria. URL: https://www.R-project.org/.

Ramos, A.M., dos Santos, L.A.R., Fortes, L.T.G., 2009. Normais climatológicas do Brasil, 1961-1990. Instituto Nacional de Meteorologia-INMET, Ministério da Agricultura.

Tompalski, P., Coops, N.C., White, J.C., Goodbody, T.R., Hennigar, C.R., Wulder, M.A., Socha, J., Woods, M.E., 2021. Estimating changes in forest attributes and enhancing growth projections: a review of existing approaches and future directions using airborne 3d point cloud data. Current Forestry Reports 7, 1–24. URL: https://doi.org/10.1007%2Fs40725-021-00135-w, doi:10.1007/s40725-021-00135-w.

Torres, D.L., Feitosa, R.Q., Happ, P.N., Rosa, L.E.C.L., Junior, J.M., Martins, J., Bressan, P.O., Gonçalves, W.N., Liesenberg, V., 2020. Applying fully convolutional architectures for semantic segmentation of a single tree species in urban environment on high resolution UAS optical imagery. Sensors 20, 563. URL: https://doi.org/10.3390%2Fs20020563, doi:10.3390/s20020563.

Torres-Sánchez, J., López-Granados, F., Serrano, N., Arquero, O., Peña, J.M., 2015. High throughput 3-d monitoring of agricultural-tree plantations with unmanned aerial vehicle (UAS) technology. PLoS ONE 10. doi:10.1371/journal.pone.0130479.

Torresan, C., Carotenuto, F., Chiavetta, U., Miglietta, F., Zaldei, A., Gioli, B., 2020. Individual tree crown segmentation in two-layered dense mixed forests from UAS LiDAR data. Drones 4, 10.

Tudoran, G.M., 2022. Using mathematical models based on unmanned aerial vehicle optical imagery to estimate tree and stand characteristics. Bulletin of the Transilvania University of Braşov 15. URL: https://doi.org/10.31926/but.ens.2022.15.64.1.5,doi:10.31926/but.ens.2022.15.64.1.5.

Tudoran, G.M., Dobre, A.C., Cics,a, A., Pascu, I.S., 2021. Development of mathematical models for the estimation of dendrometric variables based on unmanned aerial vehicle optical data: A romanian case study. Forests 12. URL: https://www.mdpi.com/1999-4907/12/2/200, doi:10.3390/f12020200.

Veras, H.F.P., Ferreira, M.P., da Cunha Neto, E.M., Figueiredo, E.O., Corte, A.P.D., Sanquetta, C.R., 2022. Fusing multi-season UAS images with convolutional neural networks to map tree species in Amazon forests. Ecological Informatics 71, 101815. URL: https://doi.org/10.1016%2Fj.ecoinf.2022.101815, doi:10.1016/j.ecoinf.2022.101815.

Yan, W., Guan, H., Cao, L., Yu, Y., Gao, S., Lu, J., 2018. An automated hierarchical approach for three-dimensional segmentation of single trees using UAS LiDAR data. Remote Sensing 10. URL: https://www.mdpi.com/2072-4292/10/12/1999, doi:10.3390/rs10121999.

GENERAL CONSIDERATIONS

According to the results obtained in this thesis, it is possible to affirm that there were positive contributions to improve the remote forest inventory commercial using the combination of high resolution images captured by UAS with deep learning methods, in particular convolutional neural networks (CNN).

Chapter I discusses the results of using CNN to identify tree species in the Amazon rainforest through aerial UAS images from different periods and their fusion, constituting a combination of powerful tools which allow mapping large areas, which are extremely difficult to access at a low cost. It is important to highlight that the methodological procedure proposed in this study is considered one of the best options for classifying forest species in environments as heterogeneous as the Amazon. This methodology provides preliminary information regarding the diversity of commercial species in the region, reducing the sampling effort in the field, making it possible to analyze the feasibility of conservation projects or forest management more quickly.

The CNN algorithm allows necessary adjustments and adaptations for application in other forests of different typologies. It is important that the tool is popularized, as it will contribute to form a library of samples and reference data (one of the challenges of this study), since the availability of samples is quite variable between species; therefore, it is important for CNN to be able to learn the different characteristics present in the species group during phenophases, and be able to apply neural network learning in other areas. The cost of the machine is high, so there is a limitation in hardware, as the combination of CNN and UAS requires powerful GPUs capable of performing all the miles of necessary interactions that the neural network needs.

Chapter II addresses a methodology for indirect biometrics of trees through the canopy using aerial UAS images, constituting valuable information which helps in planning forest management or conservation projects, since this study brings estimates of the volumetric stock of a forest by diameter class. These are crucial attributes that the environmental manager needs to support decision-making, in turn optimizing financial resources and time.

Future studies will be able to concentrate on applying this methodology in different forests to evaluate the level of accuracy, and it will also be possible to fit the models to compose biometrics of samples where the crown does not have leaves; this characteristic was excluded from this study because it generates noise in the estimates. Improve the modeling so that it can

fully portray the biometrics of the forest diameter classes is a problem which currently exists in large individuals present in the upper diameter classes

Finally, it can be considered that the hypotheses of this study were met and that the use of aerial images in forest planning can bring valuable technical and scientific contributions to the conservation of the Amazon forest.

GENERAL CONCLUSION

According to the proposed methodology and the results obtained in this study, it is possible to conclude that:

- Aerial images from the UAS with high spatial resolution, combined with the use of CNN enable discriminating forest species commercial in the Amazon.
- The fusion of multi-station aerial images of the UAS applying CNN improves the classification accuracy of forest species commercial, therefore the neural network can learn different characteristics (ecological phenophases) present in the species over the course of months.
- The diameter and crown area variables obtained by aerial images from the UAS have a strong relationship with the DBH and the basal area of the tree, and are relevant variables in estimating the preliminary commercial volume (m^3) in native forest areas in the Amazon.
- The volumetric model derived from combining diameter and canopy area generated promising estimates at low cost, making it possible to have preliminary knowledge of the commercial tree stock present in the forest.

GERAL REFERENCES

de Almeida, D.R.A., Broadbent, E.N., Ferreira, M.P., Meli, P., Zambrano, A.M.A., Gorgens,E.B., Resende, A.F., de Almeida, C.T., do Amaral, C.H., Corte, A.P.D., Silva, C.A., Romanelli, J.P., Prata, G.A., de Almeida Papa, D., Stark, S.C., Valbuena, R., Nelson, B.W., Guillemot, J., Féret, J.B., Chazdon, R., Brancalion, P.H., 2021. Monitoring restored tropical forest diversity and structure through UAS-borne hyperspectral and LiDAR fusion. Remote Sensing of Environment 264, 112582. doi: 10.1016/j.rse.2021.112582.

de Almeida Papa, D., de Almeida, D.R.A., Silva, C.A., Figueiredo, E.O., Stark, S.C., Valbuena, R., Rodriguez, L.C.E., d' Oliveira, M.V.N., 2020. Evaluating tropical forest classification and field sampling stratification from LiDAR to reduce effort and enable landscape monitoring. Forest Ecology and Management 457, 117634. doi: 10.1016/j. foreco.2019.117634.

da Costa, M.B.T., Silva, C.A., Broadbent, E.N., Leite, R.V., Mohan, M., Liesenberg, V., Stoddart, J., do Amaral, C.H., de Almeida, D.R.A., da Silva, A.L., Goya, L.R.R.Y., Cordeiro, V.A., Rex, F., Hirsch, A., Marcatti, G.E., Cardil, A., de Mendonça, B.A.F., Hamamura, C., Corte, A.P.D., Matricardi, E.A.T., Hudak, A.T., Zambrano, A.M.A., Valbuena, R., de Faria, B.L., Junior, C.H.S., Aragao, L., Ferreira, M.E., Liang, J., de Pádua Chaves e Carvalho, S., Klauberg, C., 2021. Beyond trees: Mapping total aboveground biomass density in the brazilian savanna using high-density UAS-LiDAR data. Forest Ecology and Management 491, 119155. doi: 10.1016/j.foreco.2021.119155.

da Cunha Neto, E.M., Rex, F.E., Veras, H.F.P., Moura, M.M., Sanquetta, C.R., Käfer, P.S., Sanquetta, M.N.I., Zambrano, A.M.A., Broadbent, E.N., Corte, A.P.D., 2021. Using high-density uas-LiDAR for deriving tree height of araucaria angustifolia in an urban atlantic rainforest. Urban Forestry Urban Greening 63, 127–197. doi: 10.1016/j.ufug.2021.127197.

d'Oliveira, M., Broadbent, E., Oliveira, L., Almeida, D., Papa, D., Ferreira, M., Zambrano, A., Silva, C., Avino, F., Prata, G., Mello, R., Figueiredo, E., Jorge, L., Junior, L., Albuquerque, R., Brancalion, P., Wilkinson, B., da Costa, M.O., 2020. Aboveground biomass estimation in Amazon tropical forests: a comparison of aircraft- and GatorEye UAS-borne LiDAR data in the chico mendes extractive reserve in acre, brazil. Remote Sensing 12, 1754. doi: 10.3390/rs12111754.

d'Oliveira, M.V.N., Figueiredo, E.O., de Almeida, D.R.A., Oliveira, L.C., Silva, C.A., Nelson, B.W., da Cunha, R.M., de Almeida Papa, D., Stark, S.C., Valbuena, R., 2021. Impacts of selective logging on amazon forest canopy structure and biomass with a LiDAR and photogrammetric survey sequence. Forest Ecology and Management 500, 119648. doi: 10. 1016/j.foreco.2021.119648.

Ferreira, M.P., de Almeida, D.R.A., de Almeida Papa, D., Minervino, J.B.S., Veras, H.F.P.,1 Formighieri, A., Santos, C.A.N., Ferreira, M.A.D., Figueiredo, E.O., Ferreira, E.J.L., 2020. Individual tree detection and species classification of Amazon palms using UAS images and deep learning. Forest Ecology and Management 475, 118397. doi: 10.1016/j.foreco.2020.118397.

Ferreira, M.P., Lotte, R.G., D'Elia, F.V., Stamatopoulos, C., Kim, D.H., Benjamin, A.R., 2021. Accurate mapping of brazil nut trees (*Bertholletia excelsa*) in Amazon forests using worldview-3 satellite images and convolutional neural networks. Ecological Informatics 63, 101302. doi: 10.1016/j.ecoinf.2021.101302.

Ferreira, M.P., Wagner, F.H., Aragão, L.E., Shimabukuro, Y.E., de Souza Filho, C.R., 2019. Tree species classification in tropical forests using visible to shortwave infrared WorldView-3 images and texture analysis. ISPRS Journal of Photogrammetry and Remote Sensing 149, 119–131. doi: 10.1016/j.isprsjprs.2019.01.019.

Figueiredo, E.O., d'Oliveira, M.V.N., Braz, E.M., de Almeida Papa, D., Fearnside, P.M., 2016. LIDAR-based estimation of bole biomass for precision management of an Amazon forest: Comparisons of ground-based and remotely sensed estimates. Remote Sensing of Environment 187, 281–293. doi: 10.1016/j.rse.2016.10.026.

Hartley, R.J.L., Leonardo, E.M., Massam, P., Watt, M.S., Estarija, H.J., Wright, L., Melia, N., Pearse, G.D., 2020. An assessment of high-density UAS point clouds for the measurement of young forestry trials. Remote Sensing 12, 4039. doi: 10.3390/rs12244039.

Kuzmin, A., Korhonen, L., Kivinen, S., Hurskainen, P., Korpelainen, P., Tanhuanpää, T., Maltamo, M., Vihervaara, P., Kumpula, T., 2021. Detection of european aspen (*Populus tremula* l.) based on an unmanned aerial vehicle approach in boreal forests. Remote Sensing 13, 1723. doi: 10.3390/rs13091723.

Lahssini, K., Teste, F., Dayal, K.R., Durrieu, S., Ienco, D., Monnet, J.M., 2022. Combining LiDAR metrics and sentinel-2 imagery to estimate basal area and wood volume in complex forest environment via neural networks. IEEE Journal of Selected Topics in Applied Earth Observations and Remote Sensing 15, 4337–4348. doi: 10.1109/jstars.2022.3175609.

Lassalle, G., Ferreira, M.P., La Rosa, L.E.C., de Souza Filho, C.R., 2022. Deep learning-based individual tree crown delineation in mangrove forests using very- high-resolution satellite imagery. ISPRS Journal of Photogrammetry and Remote Sensing 189, 220–235. doi: 10.1016/j.isprsjprs.2022.05.002.

Leite, R.V., Silva, C.A., Broadbent, E.N., do Amaral, C.H., Liesenberg, V., de Almeida, D.R.A., Mohan, M., Godinho, S., Cardil, A., Hamamura, C., de Faria, B.L., Brancalion, P.H., Hirsch, A., Marcatti, G.E., Corte, A.P.D., Zambrano, A.M.A., da Costa, M.B.T., Matricardi, E.A.T., da Silva, A.L., Goya, L.R.R.Y., Valbuena, R., de Mendonça, B.A.F., Junior, C.H.S., Aragão, L.E., García, M., Liang, J., Merrick, T., Hudak, A.T., Xiao, J., Hancock, S., Duncason, L., Ferreira, M.P., Valle, D., Saatchi, S., Klauberg, C., 2022. Large scale multi-layer fuel load characterization in tropical savanna using GEDI spaceborne LiDAR data. Remote Sensing of Environment 268, 112764. doi: 10.1016/j.rse.2021.112764.

Ma, M., Liu, J., Liu, M., Zeng, J., Li, Y., 2021. Tree species classification based on sentinel-2 imagery and random forest classifier in the eastern regions of the qilian mountains. Forests 12, 1736. doi: 10.3390/f12121736.

Mohan, M., Leite, R.V., Broadbent, E.N., Jaafar, W.S.W.M., Srinivasan, S., Bajaj, S., Corte, A.P.D., do Amaral, C.H., Gopan, G., Saad, S.N.M., Kamarulzaman, A.M.M., Prata, G.A.,

Llewelyn, E., Johnson, D.J., Doaemo, W., Bohlman, S., Zambrano, A.M.A., Cardil, A., 2021. Individual tree detection using UAS-LiDAR and UAS-SfM data: A tutorial for beginners. Open Geosciences 13, 1028–1039. doi: 10.1515/geo-2020-0290.

Mohan, M., Silva, C., Klauberg, C., Jat, P., Catts, G., Cardil, A., Hudak, A., Dia, M., 2017. Individual tree detection from unmanned aerial vehicle (UAS) derived canopy height model in an open canopy mixed conifer forest. Forests 8, 340. doi: 10.3390/f8090340.

Moura, M.M., de Oliveira, L.E.S., Sanquetta, C.R., Bastos, A., Mohan, M., Corte, A.P.D., 2021. Towards amazon forest restoration: Automatic detection of species from UAS imagery. Remote Sensing 13, 2627, doi: 10.3390/rs13132627.

Nasiri, V., Darvishsefat, A.A., Arefi, H., Pierrot-Deseilligny, M., Namiranian, M., Bris, A.L., 2021. Unmanned aerial vehicles (UAS)-based canopy height modeling under leaf-on and leaf-off conditions for determining tree height and crown diameter (case study: Hyrcanian mixed forest). Canadian Journal of Forest Research 51, 962–971. doi: 10.1139/cjfr-2020-0125.

Novak, M., Prokysek, M., Dolezal, P., Hais, M., Gril, S., Davidkova, M., Geyer, J., Hofmann, P., Paudyal, R., 2020. Multisensor UAS system for the forest monitoring, in: 2020 10th International Conference on Advanced Computer Information Technologies (ACIT), IEEE. doi: 10.1109/acit49673.2020.9208993.

Parmehr, E.G., Amati, M., 2021. Individual tree canopy parameters estimation using UAS-based photogrammetric and LiDAR point clouds in an urban park. Remote Sensing 13, 2062. doi: 10.3390/rs13112062.

Schiefer, F., Kattenborn, T., Frick, A., Frey, J., Schall, P., Koch, B., Schmidtlein, S., 2020. Mapping forest tree species in high resolution UAS-based RGB-imagery by means of convolutional neural networks. ISPRS Journal of Photogrammetry and Remote Sensing 170, 205–215. doi: 10.1016/j.isprsjprs.2020.10.015.

You, H., Huang, Y., Qin, Z., Chen, J., Liu, Y., 2022. Forest tree species classification based on sentinel-2 images and auxiliary data. Forests 13, doi: 10.3390/f13091416.